On a Routing Network of Causal Flow and Its Reading under Relationalism

C.Y. Hsieh
Rayark Inc.

7 November 2026

Abstract

This paper builds a causal network as an explicit mathematical structure and reads physics from inside it. The network stores no coordinate, shared clock or field, and only routes causal flow along bands on the Laves graph of a three-torus. The graph is a cubic crystal net, the discrete frame for the symmetries named CP and CPT. A single irreversible event, the lock, twists every band with one handedness and leaves an extra half twist on some band ends; only at a vertex whose three band ends all carry one can flow be held and delayed, and holding gives the network's history an arrow. Swaps behind the lock's front mix the flow into a causally trivial medium, the datum of every reading: only what departs from it is nontrivial and can be read. Under coarse-graining the lattice detail of the routing becomes irrelevant and one collective mode survives, isotropic in its stride, which is fixed in cells per update. Physics enters through readers inside the network, which receive only counts of the flow passed between them and a source. An incidence transform turns the counts into an image on the reader's sky, and demodulation decodes the nontrivial part, carried on phase and frequency channels. Under conventions of scale and of relativity, with light's speed as the conversion ratio between space and time, the decoded signals read as rest mass, charge and motion. The readings span four dimensions: three from the translations of the Laves graph, time from the reader's own count, and Lorentz invariance at readout from the relativity principle. Defects move by the glide, a two-tick event of the routing machine, and the machine hands up its transport coefficients and shows what it lacks. A second, coarse machine, with declared design choices, supplies what is missing, and toy-universe experiments on it read gravitational, wave and scattering phenomena. Every claim is graded, from forced to conjectured, and since both machines are programs, every measured claim is checked by released code and records; what stays open is listed.

Keywords: emergent spacetime; pregeometry; causal network; lattice gas automata; Laves graph; relationalism

1 Introduction

Physics knows space, time and motion only through readings, a clock's ticks or a detector's counts; this paper builds the readings first, and four dimensions come out of them, with Lorentz invariance at readout (Section 5). It starts from a causal network that routes causal flow, a purely mathematical structure; a routing machine implements it for study, and nothing here claims that a machine runs it. Mathematical structure plus relation is taken to be physics, a stance named relational realism and old in physics in many forms; what this paper adds is an explicitly constructed structure for that reading to act on: all physics comes from conventional readings made by readers within it, and the structure has no defined outside.

Topology. The first part builds the structure that everything else reads (Sections 2–4). Epistemic principles, premises that the theory takes and cannot prove from within, fix its form: it stores no coordinate, no shared clock and no field. The principles select the graph, the Laves graph on a three-torus, a crystal net; each edge carries bits, and every tick each bit moves one edge along a fixed route: this is the causal flow. One irreversible event, the lock, twists every band of the net with one

handedness and leaves an extra half twist on some band ends; only at a vertex whose three band ends all carry one can a pair of bits be held, and holding gives the history an arrow. The routing machine that results, called L1, has no tunable parameter in routing, swap and hold, and the part closes with the symmetries that survive the lock. It comes first because a reader tells readings apart only through the distinguishable degrees of freedom that this topology supplies.

Reading the L1 machine. The second part puts readers inside the network (Sections 5 and 6). A reader receives only counts of the flow passed between it and a source, never a network coordinate or tick. A transform turns the counts into an image on the reader's sky, so a distance read belongs to the image, not the network, and declared conventions of rulers, clocks and the speed of light read the image as rest mass, charge and motion. A ring of readers around one held source closes this reading on the machine. Then the defects themselves move by the glide, a two-tick event of the routing machine, as in programs where particles are patterns moving over a substrate (cf. [1, 2, 3]), and the machine hands up its transport coefficients. It also shows what it lacks, inertia, a strict bound on speed, a lapse and a ruler, and that sets the third part.

The L2 machine and its experiments. The third part builds a second, coarse machine, L2, of fluid, tension and frame layers that supplies what L1 lacks (Section 7); its design choices are not derived, and each is declared as a choice. Toy-universe experiments on it (Section 8) read gravity, light, interference and scattering from the layers, each with a measured value. Section 9 discusses what has no machine yet and lists the open problems, and Section 10 concludes.

Reading guide. Sections 2 and 3 define the machine; Section 4 can be skipped on a first reading; Appendices A and B justify the construction and carry no main claim; symbols are in Appendix F.

Grades. Every claim in Sections 2–9 carries a grade in brackets, and a chain of claims takes its weakest link, in the order F, D, Sim, Rev, Conj, P. **[F]** is forced: a mathematical structure, or an exhaustive check. **[D]** is derived from **[F]** claims and known theorems or conservation laws, the theorem or premise named, so "**[D]** given X" names an upstream premise. **[Sim]** is a machine test, with its value and error; **[Rev]** is a choice among possibilities, made to match physics that the sentence names; **[Conj]** is a conjecture, held true and not shown; **[P]** is a postulate, assumed with no reason given, and none is used. **[L]** is a labelling, a physics name for a machine phenomenon, outside the order. A grade covers the claims back to the previous grade or the paragraph's start. The principles (Appendix A), definitions, this section, the opening of Section 9, its open problems (Section 9.2) and Section 10 carry none.

2 The causal network on T^3 and its symmetries

This section fixes the board, a graph whose edges carry bits, and the rule by which they move before anything breaks the symmetry; Section 3 breaks it once. Appendix A records how the epistemic principles motivate this network.

Graph. The graph of the network is the Laves graph [4], closed into the three-torus T^3, as Appendix A.3 derives from the principles. **[D]** The Laves graph is also the srs net of reticular chemistry [5], Wells' (10,3)-a [6] and Sunada's K_4 crystal [7]. Every vertex meets three edges; the vertices fall into two classes, A and B, and each edge joins A to B; the shortest cycle has ten edges. **[F]** The quotient of the Laves graph by its translations is the complete graph K_4, with first Betti number 3, and the translations form a lattice of rank 3. The same construction on the honeycomb gives the theta graph, with first Betti number 2, drawn in Fig. 1a–d as a planar analogue. **[F]** Given the Laves graph, second-order isotropy follows from the principles, through the symmetry of K_4 (Appendix A.4). **[D]** The network is the quotient of the maximal abelian cover of K_4 by translations (Appendix A.3), and its reading as flat space is in Section 9.1 (Flatness). **[D]**

Bands and registers. Each edge is a band with two sides. Each vertex carries a cyclic order of its three bands, the rotation system; numbered in this order, a band has the same number at both ends, so the bands fall into three band families, coloured in Fig. 1b. **[F]** Bits sit in entry registers, two at each end of a band, one on each side. Before the lock a bit keeps its side (Fig. 2a, b). The strand label χ, the side read against the vertex class (Appendix C.1), names the two strands χ_1 and χ_0, a route's two directions of motion; after the lock it is constant along a route. One side carries only 1s and the other only 0s. A register and its mirror partner, the register on the other side at the same vertex (Fig. 2a), therefore hold exactly one 1 between them, and every band has occupancy $\rho = 1/2$, the fraction of registers holding 1. **[D]**

Ticks and causal routes. Updates are counted by the network tick n, a local causal ordinal, not a global clock, so the updates form a partial order, the causal order; before the lock their schedule, any that respects the causal order, is a gauge, **[D]** which the asynchronous runs confirm (Appendix C.3). **[Sim]** A bit's successive updates form a chain in this order, and that chain, read on the graph, is the bit's route: the causal flow is the set of these chains. Each tick every bit crosses its vertex onto the next band, turning right or left by the side it arrives on.

Symmetries and conventions. Before the lock every update is a bijection with an exact time reversal, so the flow has no readable arrow; Section 4 lists its symmetries. **[F]** Four labels are conventions: the direction of circulation, the choice of rotation system, which class is named A and which side is named 1.

3 The lock and the routing machine

The lock. Before the lock a bit keeps its side, so its route turns the same way at every vertex and circles a face, the boundary walk the rotation system fixes; these face loops are open three-step helices about the four body diagonals $\langle 111 \rangle$ (Fig. 1g), one family per diagonal, and together they span a lattice of rank 3 (Appendix B.1). **[F]** The lock writes on every band a half twist of one handedness, $\Upsilon = \pm 1$, chosen before the lock. A bit now changes side on every band, so its turns alternate and its route runs straight (Fig. 2a, b). Each route uses two of three band families, so routes form three helix families, one along each cube axis (Fig. 1e, f), and no fourth. **[F]**

Overtwisted vertices. The lock's extra half twists are written as stops. Each half-edge, the end of a band at a vertex, carries one stop bit s, and a band e with ends u and u' carries $\tau_e = 1 + s_u + s_{u'}$ half twists of the lock's handedness. An overtwisted vertex is one whose three half-edges are all stopped, and at rest every stop belongs to such a triple, so τ_e is 1, 2 or 3 as none, one or both ends of e are overtwisted (Fig. 2c). **[F]** A bit arriving at an overtwisted vertex reaches the other register and turns the other way: its route turns a third of a turn into another helix family (Fig. 1c), or, through two adjacent overtwisted vertices, turns twice in opposite senses and shifts by one row (Fig. 1d). **[F]** An overtwisted vertex is called a seat for what it holds and a defect for how it moves: the two words name one object, and only seats can hold and unhold a pair (Appendix A.5). **[F]** Defects move by the glide of Section 6, which moves stops and never cuts or reglues a band. Their pattern at the lock is primordial data, and no law below assumes a particular pattern. Whatever the lock's rule, the pattern is discrete with finite mean density. **[F]** It is taken statistically uniform above some scale and aperiodic, unlike the pattern with every A vertex overtwisted, to match a homogeneous, isotropic space. **[Rev]** As an ensemble it is balanced over the four orientations of the threefold axes, lest its rest frame be preferred. **[Rev]** Rates and readings do depend on it, as the loss of lattice momentum to the overtwisted vertices shows (Section 5.2). **[Sim]**

Swap and hold. A swap, which lets a pair of bits cross a band as if it were untwisted, needs a twisted band, so swaps exist only after the lock. **[F]** The twisted region is thus a new phase. Any twisted band is a venue, a band where a swap can fire (Appendix B.1). **[D]** The lock gives the machine its two events: a swap, which mixes the flow and sets its clock, and a hold, which delays it and will read as mass. A swap fires in the only two occupancies of a twisted band where crossing as if untwisted changes the outcome but no strand count; no record shows which bit continued which. **[F]** On a product state at $\rho = 1/2$ swaps fire at $1/8$ per band per tick, the clock. **[D]** On the mixed state below the run gives 0.12501 ± 0.00004. **[Sim]** A seat holds a pair and unholds it on its entry band, delayed, or on another band, turned (Fig. 2d); the delay is chosen to read as rest mass. **[Rev]** Each tick conserves both strand counts. No rule of routing, swap or hold has a tunable parameter. **[D]**

The tick after the lock, and its arrow. The lock adds two events to the tick of Section 2: the hold, in which an empty seat holds a pair arriving on mirror registers and unholds it once both registers of the exit band are empty, and the swap; then the free bits move as before. The order of phases within a tick is a declared choice (Appendix C); the schedule of updates over vertices, with holds and swaps on, is still a gauge (Appendix C.3). The blocked advance of a held pair's exit band is the one step that forgets its entry band, so a held state has several pasts and the update has no inverse at a seat (Appendix B.1); these merges write the arrow on the transient the lock starts, before the finite system enters its final cycle. **[F]**

Mixing into the CTM. The lock leaves the flow in a mixed state, the causally trivial medium (CTM): a state of the flow, not stored structure, which no rule refers to. Every later reading is a departure from it. Behind the front of the twist, 99.2% of the content at a band is mixed 8 ticks after its arrival, and each side's composition settles at $1/2$ plus an offset $\delta = (-5.3 \pm 0.3) \times 10^{-4}$ (Appendix B.1); to this order the CTM is a uniform product state, which the readings below take as premise, and it

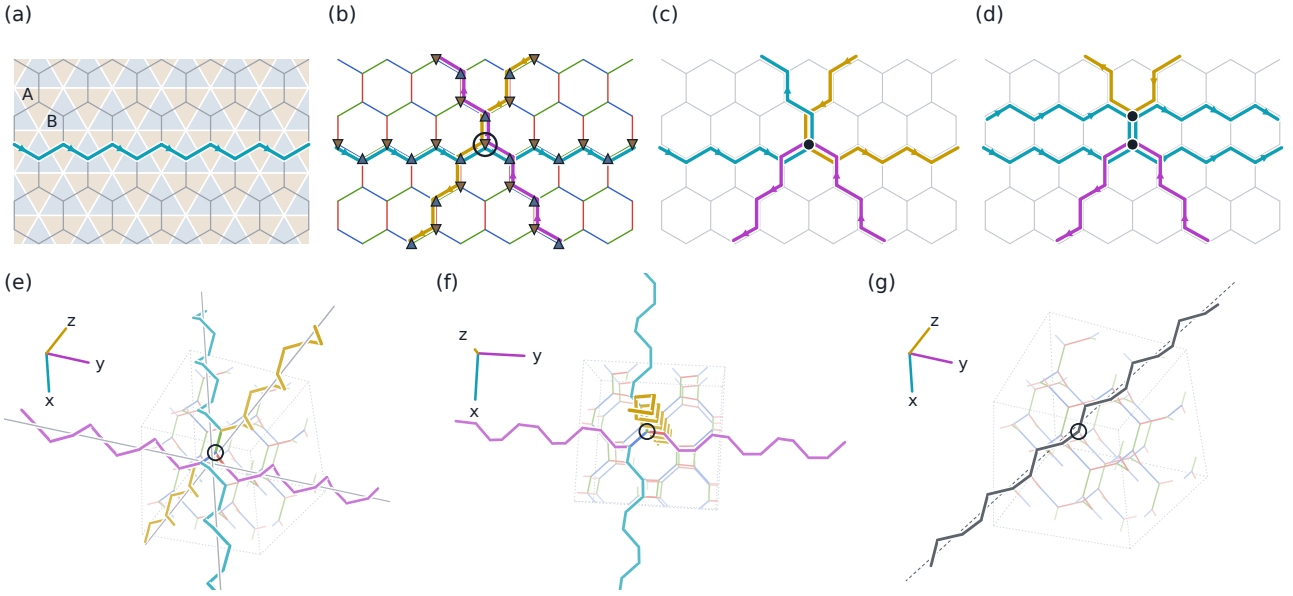


Figure 1: Routes under the rule of the Laves graph, on the honeycomb, (a)–(d), in the plane only for readability, and on the Laves graph, (e)–(g). A ring marks the vertex the routes pass through, a black dot an overtwisted vertex. (a) Vertices at the centres of dual triangles, A down (warm grey), B up (cool grey). (b) Bands coloured by band family (red, green, blue), triangles marking the classes as in (a); each route takes the additive mix of the two families it alternates between. (c) An overtwisted vertex. (d) An adjacent overtwisted A–B pair. (e) Routes along the cube axes, coloured as the axis marker; grey lines, the helix axes. (f) The view of (e) about 6° off one axis. (a)–(f) are routes after the lock; (g) is one before it, in the view of (e): a face loop advancing one body-centring vector per period along a body diagonal (dashed).

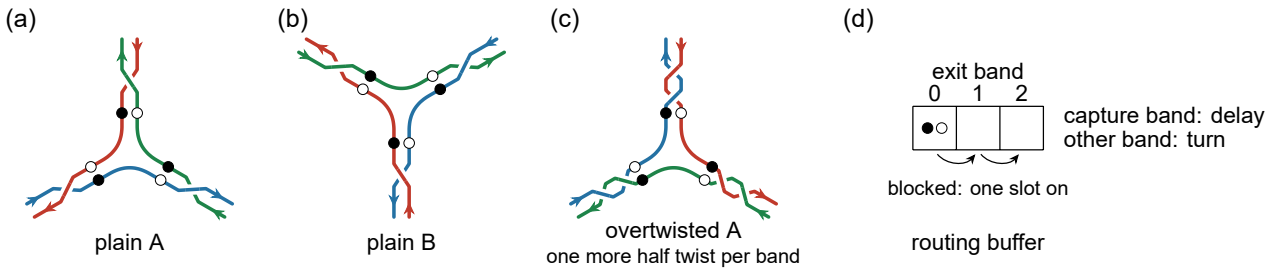


Figure 2: Bands at a vertex. Each stub is half a band; its two sides cross once at the band's midpoint, the lock's half twist. Each side carries χ_1 along its arrow and χ_0 against it; filled and open dots are the χ_1 and χ_0 entry registers. (a) Plain A vertex: χ_1 turns right. (b) Plain B vertex: χ_1 reversed, turns left. (c) Overtwisted A vertex, one more half twist per band: χ_1 reaches the open dot and turns left, one exchange of strands relative to (a). (d) A seat's routing buffer, indexed by the held pair's exit band.

carries no signal of its own: a reader on it reads the reference, up to noise. **[Sim]** The mixing rests on two declared choices, the phase order, in which swap detection runs before routing and so sees a new twist a tick later, and the lock as a front that crosses the network: content is unprotected at each band's first twisted crossing, and a twist written everywhere at once, with or without overtwisted vertices, would not mix (Appendix B.1). **[D]** A run of such a twist leaves 0% of the content mixed. **[Sim]**

4 Discrete symmetries after the lock

The lock leaves three tiers of discrete symmetry: operations exact with holds, operations exact only on the defect-free CTM, and a static invariant of the bands. Exactness here means that an operation maps every local rule table to itself, checked vertex type by vertex type; the proofs, the counts and the full sign ledger are in Appendix B.3, and this section says what each tier is read as. Section 5 names machine operations C, P, T, a charge sign and helicity, and those names may attach only to exact operations; Table 1 and Eq. (1) list the operations the readings use.

Exact with holds. Four operations each reverse the turning of every hold, and so break alone at the seats: the body-centre translation t_{bc}, which exchanges the two vertex classes; the fourfold screw rotation Rot_4; the twofold rotation Rot_2 about a face diagonal; and Mir, which reverses the rotation system at every vertex and keeps every position and half twist. **[F]** A product of an even number of them restores every hold and is exact bit by bit, as are the translations by whole cells, the threefold rotation about a body diagonal and the twofold rotation about a cube axis. **[F]** The parity law: of an operation and its image under Mir, exactly one is exact with holds, so Mir is seen only through overtwisted vertices; with none, both are exact. **[F]** The complement X, which exchanges 0 and 1, breaks at the seats, since holds take only 1s. The exact product $t_{\mathrm{bc}} \circ \mathrm{Rot}_4$ flips every side, keeps every strand and maps the state before the lock to its complement, so which side is named 1 is carried by an exact symmetry; it stays exact while the lock's front crosses the network. **[F]** The handedness Υ of the lock's half twists is read, not broken: the class exchange composed with the diagonal mirror $\sigma_d = \mathrm{Inv} \circ \mathrm{Rot}_2$, with Inv the point inversion of the embedding, reverses it and is exact with holds, while the mirror alone breaks, so the lock is written alike from either seed class at either handedness. **[F]**

Rotations of a held source. The operations that break at the seats include proper rotations, Rot_4 and Rot_2, so a held source turned by Rot_4 is not a held state, and the exact $t_{\mathrm{bc}} \circ \mathrm{Rot}_4$ turns it into its conjugate, of opposite charge: not the same source. **[F]** A source of given charge and turning therefore occurs in the 12 orientations of the turning-keeping proper rotations, the identity, the eight threefold rotations about $\langle 111 \rangle$ and the three twofold rotations about the cube axes (Rot_4^2), the chiral tetrahedral group T; the other 12 give its conjugate. **[F]** This group acts irreducibly on directions, so the

Operation	Named	With holds
t_{bc}	C	breaks
σ_d	P (a choice)	breaks
J_{state}	T, Wigner's reversal of motion	in distribution
$t_{\mathsf{bc}} \circ \sigma_d$	CP	exact
$t_{\mathsf{bc}} \circ \sigma_d \circ J_{\mathsf{state}}$	CPT	in distribution
X	which side is named 1	CTM only
$t_{\mathsf{bc}} \circ \mathsf{Rot}_4$	the exact flip of every side	exact

Table 1: Operations and the names the readings give them: exact with holds, in distribution, or exact only on the defect-free CTM; the full sign ledger is Table 5. **[F]** The in-distribution rows are a simulation claim. **[Sim]**

second-order readings of a held source are isotropic, by Schur's lemma as in the isotropy argument of Appendix A.4; **[D]** differences between orientations at fourth order are not claimed.

Read-as names. The translation t_{bc} is named C and the state reversal J_{state} T; naming σ_d P is a choice. **[L]** Hence CP is $t_{\mathsf{bc}} \circ \sigma_d$ and CPT is $t_{\mathsf{bc}} \circ \sigma_d \circ J_{\mathsf{state}}$. **[L]** Since Inv changes no label the rules read (it reverses only the embedding labels Υ and h; Appendix B.3), CP acts on the machine as $t_{\mathsf{bc}} \circ \mathsf{Rot}_2$, exact with holds, and CPT is exact on the defect-free CTM. **[F]** With holds, CPT holds in distribution. **[Sim]**

Reversal. The state reversal J_{state} sends each register across the band its bit leaves by and keeps the class, so that side 1 is side 0 run backwards; it is an involution that sends each routing table to its inverse, and on the defect-free CTM it is exact as a reversal. **[F]** This paper takes it to pair the two strands on a band: χ_0 is χ_1 run backwards, Wigner's reversal of motion. **[L]** With holds on, J_{state} still matches the forward run in distribution: the occupancy per overtwisted vertex differs by $(-1.2 \pm 0.4) \times 10^{-4}$. **[Sim]** Causal reversal J_{hist}, the inverse of the update, does not exist at a seat (Section 3), so these reversals fail trajectory by trajectory, and the reversal available to the readings is J_{state}. **[F]**

Framing. Bands also carry a framing, set by their half twists in the band embedding, which no rule reads away from seats; Appendix B.1 gives it, the total-framing identity, its integer and sign layers and the events that change it (Fig. 6c). **[F]**

The forced consequence. The exact $t_{\mathsf{bc}} \circ \mathsf{Rot}_4$ sends (q, h) to $(-q, h)$, with q the route-charge sign, which transforms as the turning number w (Table 5), and h the sign of a route's band rotation, so the machine's laws give, over any ensemble that weights each pattern of overtwisted vertices like its image, the law-level zero

$$\langle q \cdot h \rangle = 0. \tag{1}$$

A pattern of overtwisted vertices may correlate q with h, but its image under $t_{\mathsf{bc}} \circ \mathsf{Rot}_4$, run by the same rules, carries the opposite correlation. **[F]** Reading a correlation of q with h, as the weak interaction's chirality, belongs to the readout layer and is left open (Section 9.2). **[L]**

5 Reading under relationalism: statics and kinematics on L1

This section states the relativity principle, builds the reader's transform, derives the static and kinematic readings in formulas, and closes with one run of the routing machine of Section 3, here called L1, read by a ring of near and far readers.

5.1 The relativity principle and the reader

A closure is a closed route through overtwisted vertices; it can hold and count, and serves as a reader or a source. A reading is a function of the flow that reaches the closure, counted in the closure's own ordinal; that is what "inside the network" means here: the inputs are the closure's own data, not that the computation runs inside it. The incidence transform below states what those arrivals determine, and in the machine the counter is an implementation convention (Appendix C). Readings of fluctuations, statistics and bunching are further readings of the same arrivals.

The relativity principle. A reading is relational in two ways. Along one object's own ordinal it relates a present window to a past one: dynamics is this relation. Between two objects it relates the windows of a source and of a reader, each counted in its owner's ordinal: a frame is this relation. Together a reading relates four windows, the present and the history of the source and of the reader (Fig. 3a), the quaternary relation. The relativity principle is relationalism (Section 1) applied to these relations: a reading uses only the causal flow passed between the four windows, never a network tick or a place on the network. What a source emits is determined by its own history alone, and a reader compares what arrives only with its own history; neither knows the other's place or history. Readers and sources of one kind are interchangeable: this is the working form of the relativity principle, the fourth principle of Appendix A.1. The static reading is the binary limit in which the source's history freezes into structure and the reader's window grows without bound (Fig. 3b). **[D]** The CTM is the datum of every reading, not a frame in one: a reading reads what differs from it. **[D]** Reading a causal structure as physics needs conventions, since mathematics alone fixes no physical reading. Four fix what counts: (i) a count is read at the frequency of the carrier that delivers it; (ii) a measurement compares with a recurrence; (iii) a reader is a closure with its own ruler; and (iv) energy is the reduced Planck constant $\overline{h}$ times a count times the clock, the CTM's single swap rate. They are chosen to match how physics reads clocks, detectors and energy. **[Rev]**

Relativity at readout. Lorentz invariance is not a property of the causal network, which has no time, length or scale of its own. The network does have a rest frame, the CTM's, and the relativity principle makes it unreadable; the zero-drag theorem below supports this for objects at any stride over a floor at rest, **[F]** and drifting floors are not claimed. Given the interchangeability of readers and sources of one kind and one convention, light's speed c_0 as the conversion ratio between space and time for every reader, radar reciprocity gives the rate law and the full Lorentz transformation at readout, as in Bondi's k-calculus [8] and as from Einstein's two postulates [9]; length contraction is no separate claim. **[D]** Time dilation is therefore a reading given the principle, not a property of causal flow; this differs from Lorentz invariance as an infrared fixed point of dynamics [10] and from causal sets, whose order is embedded in spacetime and so must be Lorentz invariant itself [11]. **[D]** A reading's speed is parametrised as $\beta = |\tanh\varphi|$ in units of c_0, φ the rapidity, the conversion ratio of the readout

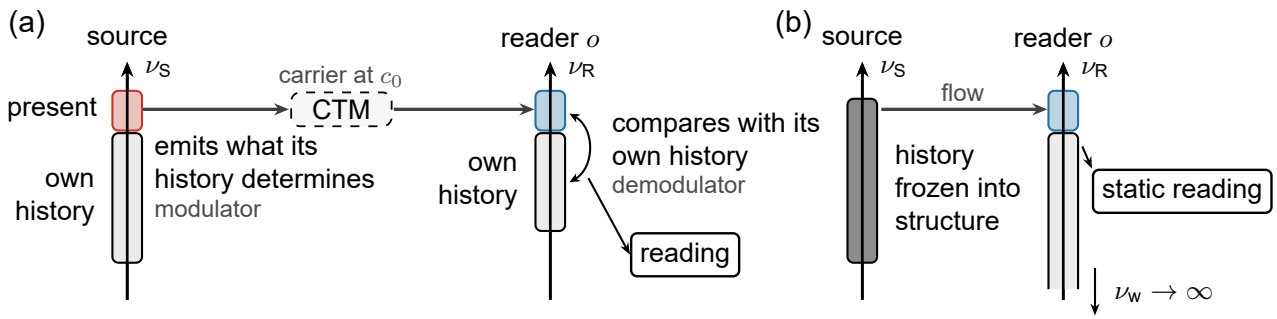


Figure 3: The quaternary relation. (a) What the source emits is determined by its own history, and the reader compares what arrives only with its own; the four windows meet only through the flow, each present a short window, not an instant; ν_s and ν_r are each owner's ordinal. (b) The static reading, the binary limit: the source's history frozen into structure, the reader's history window unbounded.

Channel	Sensitive to	Named	Grade
$\lambda = 0, \omega = 0$	counts, dwell, the $1/r$ static offset	rest mass; the potential	**[L]**
$\lambda = 1/2, \omega \to 0^+$	turning signs on the double cover	helicity h, with the closure sign $(-1)^w$; charge from w	**[L]**
$\lambda = \pm 1, \omega \neq 0$	first harmonic of the fibre angle	light's two polarisations	**[L]**
$\lambda = \pm 2, \omega \neq 0$	second harmonic of the fibre angle	gravitational radiation	**[L]**

Table 2: Channels by demodulation frequency ω and phase weight λ; w is the turning number of a closure, whose overtwisted A and B vertices differ by $3w$ (Appendix B.3), and q transforms as w.

convention. The speed c_0 is the stride of the continuous collective mode on the CTM. **[D]** Bits faster than c_0 exist on L1: a single bit runs at $\sqrt{3}\, c_0$ (Eq. (3)). **[F]** Yet a single bit's arrival is not a signal: only a window of the transform below turns arrivals into a reading. Given the Laves graph and the principle, the four dimensions come out of the reading: three from the translations of the Laves graph, a lattice of rank 3 (Appendix A.4), time from the reader's own ordinal, and the Lorentz group, acting on the two together, from the relativity principle with the c_0 convention. **[D]**

Readers and the windowed transform. A reader is a seated closure counting arrivals in its own ordinal ν. Its window is one-sided and exponential, $w(m) \propto e^{-m/\nu_{\mathrm{w}}}$ for $m \geq 0$ and zero before, in the reader's own steps, and the transform of its counts $n(\nu)$ at frequency ω is

$$X(\omega, \nu) = \sum_{m \geq 0} w(m)\, n(\nu - m)\, e^{-i\omega m}. \tag{2}$$

Five steps build it, and each carries its own grade. (1) The time axis is the reader's own ordinal, since a network tick is barred by the relativity principle. **[D]** (2) The window is finite and one-sided, since the reader's memory is finite and a reading follows its arrivals. **[D]** (3) The reading is linear in the counts: for a weak signal in local equilibrium, the premise of c_0 below, with the CTM a product state to the offset of Section 3, it is the leading reading and a sufficient one, and superposition follows (Appendix E.1). **[D]** (4) One window serves all frequencies, to match a time-frequency reading, which relationalism does not supply. **[Rev]** (5) The reader's own ruler sets its units. **[Rev]** The transform as a whole takes its weakest link, step 4. **[Rev]** The window's shape needs no grade: window-free readings exist, and the shape is stated once. A window must close on the event it reads: by Kac's lemma [12] the event returns on average after $1/\mu$ reader steps, μ the probability per step of the required configuration, and missing it with probability at most ε needs a window of about $\ln(1/\varepsilon)/\mu$ for independent steps; **[F]** the departure of the machine's steps from independence is not measured here (Appendix E.1).

The incidence transform. The transform reads three data of an arrival against three conjugates: the arrival ordinal against a frequency ω, whose group delay gives depth; the place across the reader against a wave vector, whose direction is a point of the reader's sky, the sphere S^2 of directions of the flow lines through it; and the rotation of the arrival frame about that direction, its fibre angle, against the phase weight λ, a label of the channel. **[L]** On the network $\theta = \pm 2\pi/3$ is a route's change of direction at a vertex, not the fibre angle, so λ counts only modulo 3, and $\lambda = 1/2$ only through the double cover; at the reader λ is a harmonic of the continuous fibre angle. **[F]** Table 2 lists the channels.

Names. Beyond the names C, P and T of Section 4, the band-rotation sign h is named helicity, the route-charge sign q the sign of charge, and the phase weight λ the spin weight of a readout channel: 0 for a scalar, $1/2$ for a spinor, 1 for a transverse vector, 2 for a tensor. **[L]**

The sky and the Hopf fibration. Coarse-grained at the reader, the set of directions of the flow lines is read as the sphere S^2, chosen to match the continuous sky of observation. **[Rev]** A direction with a fibre angle about it is a rotation, a point of $\mathrm{SO}(3)$, and the double cover of $\mathrm{SO}(3)$ is $\mathrm{SU}(2) = S^3$, with $S^3 \to S^2$ the Hopf fibration. **[D]** On the network the two-sheeted cover is the $\mathrm{SU}(2)$ spin lift of the band frame transport through the half twists, with holonomy $(-1)^{|C|/2}$ around a cycle C: cycles with $|C| \equiv 2 \bmod 4$, all ten-rings among them, lift open, so the cover is connected; the cover by sides alone is trivial, since every cycle of a bipartite graph is even. **[F]** The register frames of the network lift to a discrete $\mathrm{SU}(2) \to \mathrm{SO}(3)$, a nonsplit double cover of the octahedral group, so a 2π rotation built from an exact symmetry acts as -1 on $\lambda = 1/2$, and the Hopf map sends the lifts onto the 12 arrival directions with a discrete fibre $\mathbb{Z}_4$ (Appendix B.2). **[F]** After coarse-graining the arrival frames over the sky therefore form the Hopf fibration. **[D]** Neither the sphere nor a continuous fibre angle exists on the network, and a continuous λ needs the coarse-graining too. **[F]**

5.2 The static and kinematic readings

The floor the readings stand on. Readings are departures from the floor, the coarse-grained CTM; its one propagating mode, which carries every signal below, comes first. Along each route family the number and the strand difference are each other's current, so the lattice momentum flux is diagonal, and linear flow under it has one collective mode, the sound mode of lattice gases [13, 14], with stride

$$c_0 = v_{\mathrm{bit}}/\sqrt{3}, \tag{3}$$

v_{bit} the bit stride, one cell per four-tick helix turn. **[D]** Given local equilibrium about the stationary measure of a drift, the stride along a unit wavevector is set by the occupancies of the route families, Eq. (16) of Appendix E.1, so at rest the stride is c_0 in every direction, in line with the second-order isotropy of Appendix A.4. **[D]** The machine gives $c_0 = 0.14432 \pm 0.00012$ along $\langle 100 \rangle$, 0.14434 ± 0.00008 along $\langle 110 \rangle$ and 0.14439 ± 0.00009 along $\langle 111 \rangle$ cells per tick, isotropic to $0.27\% \pm 0.06\%$, against $v_{\mathrm{bit}}/\sqrt{3} = 0.14434$ (Appendix D.2). **[Sim]** The mode is isotropic in stride and anisotropic in damping: overtwisted vertices damp it, with isotropic and cubic damping $\nu_0 = 0.01084 \pm 0.00009$ and $\nu_1 = 0.0387 \pm 0.0004$ and dispersion $\varsigma = 0.0098 \pm 0.0012$, which the readings below use. **[Sim]** A drifting causal flow loses lattice momentum, the momentum of the flow along the routes, to the overtwisted vertices at $0.141 \pm 0.002\, p$ per tick with holds off and $0.200 \pm 0.001\, p$ with holds on, p their density, the rate per p staying within 4% of these values for p from 0.005 to 0.04 on a 16-cell torus. **[Sim]** Two facts of the CTM matter for what follows. A test body is a closure carried by hand through the CTM, and drag is the mean lattice momentum that the CTM takes up per tick from it.

Theorem 1 (zero drag)**.** *On the CTM itself, with the uniform product measure at $\rho = 1/2$, any reversible, number-conserving dynamics of an object without holds has mean drag exactly zero at any stride.*

With fixed routing each tick is a number-conserving bijection, which preserves the uniform product measure, so the expected change of the lattice momentum vanishes. **[F]** The same holds in frequency: on the CTM itself, any reversible, number-conserving variation of the routing at overtwisted vertices writes no phase-locked line in the spectrum of the mean occupancy, since a phase-locked line, like drag, can be written only by an irreversible unhold, the end of a hold. **[F]** The machine drags only through an irreversible unhold, at 0.18 of its gross exchange, and writes a phase-locked line only with holds, at 27.7 standard errors. **[Sim]**

Mass: the first time moment. A source holds content, and a held pair delays the flow by its dwell; by Little's law the held store is $H =$ rate times mean dwell, the first time moment of the dwell, and it adds over held pairs whatever the shape of the source. **[D]** Each held pair is a hold and an unhold in time, so its source in the floor's damped wave equation has no zeroth time moment, the number

being conserved, and its first time moment is $\tau\,\delta^3(\mathbf{x})$ for a dwell τ. For the floor's count density u responding linearly, the first time moment $S_1 = \int t\,u\,dt$ then obeys

$$-c_0^2\nabla^2 S_1 = H\,\delta^3(\mathbf{x}), \tag{4}$$

whose solution is $S_1 = H/(4\pi c_0^2 r)$ (Appendix E.1), so the reading of a source at distance r obeys

$$r\,S_1 \to \frac{H}{4\pi c_0^2}, \tag{5}$$

flat in r, the strength of Gauss's law with no free parameter. **[D]** The premise is the linear response of the floor, and the result holds up to the damping's range, which the window must outrun. Rest mass reads as this store times the clock. **[L]**

Charge: the slope. Mass came from the first time moment of the count channel ($\lambda = 0$); charge is the first-order term in λ of the spinor channel ($\lambda = 1/2$) at $\omega \to 0^+$, the limit an antenna can reach. On L1 the charge reading is screened; this paragraph fixes only its sign, and the long-range law is that of the second machine (Section 7). A hold that only delays writes no static charge, since it changes a reading only at first order in ω. **[F]** A turn gives the flow the phase $e^{i\lambda\sigma_v 2\pi/3}$, with σ_v the class sign of the vertex, which expanded to first order in λ is imaginary and odd under C. A source and a reader each respond with a $\lambda = 1/2$ turn, imaginary at first order with the sign of its route charge, and the composed reading multiplies the two, so its sign is

$$\mathrm{sgn} = -\,q_{\mathrm{s}}\,q_{\mathrm{r}}, \tag{6}$$

with q_{s} and q_{r} the route-charge signs of source and reader (Appendix E.1). **[D]** Taking the composed reading, by choice, as minus the interaction energy, like charges repel (Appendix E.1). **[Rev]**

Motion: the rate law and the Heaviside field. Two models stand in for the carrier: the transmission-line model, the lossless low-k limit of the floor's mode, which carries a source's signal to a reader at stride c_0, and the walk model, a damped, partly diffusive walk.

Proposition 1 (dynamical readers and sources)**.** *Suppose that readers and sources are dynamical, read as moving relative to the CTM, while overtwisted vertices stay seated. (i) Each counts its own ordinal ν at $1/\gamma$ times the rate of the same reader or source at rest, with $\gamma = (1-\beta^2)^{-1/2}$. (ii) A source whose envelope changes seats shows the Doppler factor $\mathcal{D} = 1/\big(\gamma(1+\beta\,\hat{n}\cdot\hat{u})\big)$, with $\hat{n}$ the direction of observation and $\hat{u}$ that of the motion, the conformal factor of the Möbius map of its sky. (iii) Through the transmission-line model a source moving uniformly at velocity $\mathbf{u} = \beta c_0\hat{u}$ gives the Heaviside field, centred on its present position,*

$$\varphi(\mathbf{x},t) = \frac{H}{4\pi c_0^2}\,\frac{\gamma}{\sqrt{\gamma^2(x_\parallel - \beta c_0 t)^2 + x_\perp^2}}, \tag{7}$$

so the transverse and axial potentials at equal distance from it stand in the ratio γ, there is no wake, and the field depends only on the distance in the source's rest frame.

Radar reciprocity forces (i) (Appendix E.1): one tick common to all would be a clock that no reader holds, by which a reading would depend on who moves over the network, which the relativity principle forbids. Proper counts, an isotropic c_0 and radar then give (ii), and the lossless wave equation is Lorentz covariant, which gives (iii). **[D]** A reader moving at β between static references fore and aft, each sending a carrier of frequency f_0, counts crests at the rates $f_0(1\pm\beta)$; its ordinal is defined as $\nu = \sqrt{n_+ n_-}$, the reading in which the factors fore and aft are reciprocal, as the relativity principle requires, and it then advances at $f_0\sqrt{1-\beta^2}$. **[D]** The Doppler factor is a frequency law: under the walk model the amplitude does not carry $\mathcal{D}$, so the kinematic readings are properties of the model, built into the transmission line and lost in the damped walk. **[D]** A velocity reading is the slope of a demodulated phase and is expected to agree with the drift of the delay: along a prescribed trajectory the integrated convective shift equals the difference of the static potential, with no window-retardation or dispersion term. **[Conj]**

5.3 Resolutions and continuity

Rate, clock and lapse. Three words are kept apart: a rate, a count per tick; a clock, a recurrence that a reader counts against, the CTM's swap rate being the clock; and a lapse. A clock is read only against another clock, and a lapse is a ratio of the ordinal rates of two clocks, never a rate.

Continuity is a description. What the readings call continuous is of three kinds. Parameters are exact: the ordinal is the integers and its dual a circle, so the demodulation frequency is continuous, and a group delay need not be whole ticks. **[D]** Values are below resolution: a windowed sum moves in steps of $1/N_{\text{eff}}$, with $N_{\text{eff}} = (\sum w)^2/\sum w^2$, while the CTM's own fluctuation is $0.5/\sqrt{N_{\text{eff}}}$, larger than the step by $\sqrt{N_{\text{eff}}}/2$, so adjacent values are indistinguishable and the value reads as continuous. **[D]** Counts are many: with a mean $\bar{n} \gg 1$ per resolution cell the relative fluctuation falls as $1/\sqrt{\bar{n}}$, so the count reads as a continuous intensity, by the central limit theorem. **[D]** The discrete count quantum is the limit of this reading and returns wherever a reader counts single arrivals rather than a windowed rate (Section 9.1). **[D]** The continuous description wins on brevity, not by being minimal; duality, the central limit theorem and indistinguishability explain why the compression works, without making the continuum real.

5.4 The closing check: a ring of readers

One run of L1 tests the readings. A rule-made cluster of 20 seats, a held source, sits in a bath, and closures read it at shells from near to far, $2.25 \le r \le 11.75$ cells. The reading of the shells with a window of $\nu_{\text{w}} = 8$ ticks follows the damped wave model of the floor, whose first time moment is Eq. (4), with the measured store $H = 1.61$ per seat: the ratio of the measured rS_1 to the model is 0.985 ± 0.006, the slope across the shells 0.003 ± 0.018, and the rms of the deviations 0.80 standard errors. **[Sim]** A shorter window, $\nu_{\text{w}} = 4$, is too short for the reading to close. **[Sim]** There is no lapse on L1: the closures' clocks at $r = 4$ to 12 run at the far rate, their hold rates and held fractions shifting by at most 1.2×10^{-4} and at most 2.2×10^{-5}, null within three standard errors; the lapse is built on the second machine (Section 7). **[Sim]** The same cluster is then carried at 0.438 of c_0. The cos-moment dipole of the shells is read as half the difference of the runs at $+x$ and $-x$, against a rest control at the same tick. The retarded position is excluded, at 9.6 standard errors, and the controls pass: the rest dipole against the geometry at 0.81 and the moving bias against the rest run at 1.2. **[Sim]** The measured lag fraction is 0.19 ± 0.06, against the damped wave model's 0.017, an rms deviation of 2.38 standard errors, outside the tolerance 1 ± 0.87: a miss, the lag exceeding the linear model (Appendix D.2). **[Sim]** The design of the run, the torus, replicas, batches and schedule, is in Appendix D.1.

6 Defect dynamics on L1

Section 5 read a held source at rest and on a prescribed path. This section lets the defects themselves move. A defect cannot move without dropping one constraint of Section 3; the section says which, gives the glide, and lists what the motion hands up to L2.

What motion requires. Relative motion needs uneven delay change: a change common to every depth only rescales them, which reads as cosmology (Section 9.1), so a source pattern has to change place. **[D]** Drag belongs to irreversible coupling only (Theorem 1), so a measurement of drag needs a reversible control first. **[F]** One constraint has to go, the static framing of each band. Every half-edge belongs to one band, so the total framing is $\sum_e \tau_e = E + N_{\text{stop}}$, with E the number of bands and N_{stop} the number of stops, and the machine declares every half twist beyond the first to be a stop, so this identity holds at every tick, whatever the glide does with stops. **[F]** With $\tau_e = 1 + s_u + s_{u'}$, changing a stop changes τ on its bands, so no move of a defect keeps the framing of every band fixed; the integrality of every τ_e stays as declared. At rest $N_{\text{stop}} = 3\, n_{\text{def}}$, with n_{def} the number of defects, and

a glide raises N_{stop} by 4 and lowers it by 4, so the total framing is constant except inside a glide (Appendix B.1). **[F]** Class charge separates motion from creation. The Laves graph is bipartite, so a one-bond step flips the class A or B of a vertex: a defect of nonzero class charge moves two bonds at a time, or through a transient A–B pair, and a string that changes the defect number by ± 2 is a creation. **[F]** The trivial floor reads as nothing at any velocity of an object over it, which is the relativity principle taken as premise (Theorem 1, for a floor at rest), since otherwise it would be an aether, and the front of a signal passes held content undelayed: a velocity-dependent reading comes from nontrivial content only. **[Rev]**

The glide. The unit of motion is a glide, completed in two ticks, with one bond moved per tick and the intermediate A–B pair a real state. At its start the held pair of the defect is unheld into its exit registers; the unhold is refused if they are occupied. In tick 1 the glide sets stops so that the defect spreads over the three vertices $\{v, w, v'\}$ along the step, of class charges $A - B + A = +1$; in tick 2 it completes the step at v'. The step is chosen by an exact integer decision, and a fixed rule orders ties (Appendix C). Its constants are declared choices: the contact shell, a fixed set of lattice offsets within 1.6 cells invariant under the cube group; the weights of the step ledger, one entry per dart, recording the momentum exchanged with passing bits; the threshold; and the tie rule, stated as specification only. The step ledger is a deck-class vector with the Schur-unique inner product (Appendix A.4), so no coordinate is stored. **[Rev]** Every bit and every stop moves at most one bond per tick, the class charge $q_{\text{cl}} = n_A - n_B$ is exact at every tick, the defect stays single, and the count mode and the floor are untouched. **[F]** The run counts 0 violations of the class charge in every tick of every run; the stop identity holds by declaration and the engine asserts it (Appendix C.3). **[Sim]** A seat starts a glide at the rate 0.111 per tick. **[Sim]** No pair is created on L1: creation and annihilation of defects are left to the coarse layer, since a free pair-creation rule adds no distinction that motion needs and a propagating carrier needs a nearly defect-free floor (Appendix A). **[Rev]** The glide keeps every exact symmetry of Section 4, as the equivariance of its tables there shows. **[F]** In distribution, over runs of the moving machine, the exact operations and J_{state} leave every mean unchanged: the largest standardised difference is 1.77 under Mir and 1.78 under t_{bc}, the mean F statistic 1.05, and the smallest Bonferroni-corrected p 0.71. **[Sim]**

The least move. If stops move at most one bond per tick and every stop sits in a full vertex triple at the start of the tick, a tick that moves a defect changes q_{cl} or the defect number (Appendix A.1); the least event that moves a defect and keeps both is therefore two ticks long, with stray stops only between them. **[F]**

The arrow as dissipation. The blocked advance of the buffer, a pair held on one band that leaves on another, is the only irreversibility of routing, swap and hold; away from the defects every update is a bijection, and the move phase is not shown injective, so it may merge states too. **[F]** Moving defects and the floor reach a joint steady state: over the run the floor is neither heated, polarised nor depleted. The swap rate per band changes by 4.3×10^{-5} between the first and the last window, the variance by a relative 1.1%, the polarisation by $(-1 \pm 4) \times 10^{-5}$ per bit in units of c_0, and the number N by 0; the hold fraction and the mean speed change by $(-0.3 \pm 1.4) \times 10^{-4}$ and $(-1 \pm 5) \times 10^{-5}$. **[Sim]** At the level of a seat the motion is overdamped: the velocity has the memory $\tau_v = 0.988$ ticks and is white beyond it, with no inertial regime. **[Sim]**

What L1 hands up. The hand-over quantities are defined by the motion of one defect in the joint steady state. The diffusion constant D is read from the mean square displacement, $\langle |\Delta \mathbf{x}|^2 \rangle = 6Dt$ at long times, and from the Green–Kubo integral of the velocity autocorrelation, $D = \frac{1}{3} \int_0^\infty \langle \mathbf{v}(0) \cdot \mathbf{v}(t) \rangle \, dt$; the two agree when the velocity has a memory τ_v, $\langle \mathbf{v}(0) \cdot \mathbf{v}(t) \rangle \propto e^{-t/\tau_v}$, short against the time of observation; here the displacement estimate falls with the window, 3.44×10^{-3} at 64 ticks and 3.15×10^{-3} at 256, still 3.2% above the Green–Kubo value, which L2 takes. Entrainment is the ratio of a defect's drift to the speed u of the local flow, $v = (v/u)\, u$, and the content-gradient mobility is

Quantity	Value	Role
defect diffusion D: Green–Kubo, displacement over 64 ticks and over 256 ticks	$(3.0571 \pm 0.0025) \times 10^{-3}$, $(3.4409 \pm 0.0015) \times 10^{-3}$, $(3.1548 \pm 0.0025) \times 10^{-3}$	mobility of a defect
ratio of the classes D_A/D_B	0.9983 ± 0.0018	no class asymmetry of motion
velocity memory τ_v	0.988	overdamped seat
speed, mean and rms, in c_0	0.644, 0.668	transport only, no bound
fraction at c_0, fraction above	0.0477, 0	the edge of the glide
entrainment v/u	0.0097 ± 0.0020	drift with the local flow
content-gradient drift μ_n, μ_n/D	-0.0018 ± 0.0003, -0.57 ± 0.11	down the gradient
hold fraction of a seat	0.811	held store
A–B imbalance μ_{A-B}/D	$(5.3 \pm 2.7) \times 10^{-5}$	null
static source, radial drift in c_0	$(2 \pm 4) \times 10^{-4}$	null: no static drive
class pairs $g(r)$, rms z	0.96, 0.54, 0.45	null: flat

Table 3: The hand-over table of L1: transport coefficients and nulls, all **[Sim]**.

defined by $\mathbf{v} = \mu_n \nabla n$, with n the bit content; a negative μ_n is a drift down the gradient. The imbalance $\mu_{A-B} = \mu_A - \mu_B$ of the classes' content-gradient mobilities is a null: the two classes move alike. Table 3 lists what the machine carries to the layer above, each a measured value, and its nulls. Four things are absent, inertia, a strict bound, a lapse and a ruler, and each is built where it is needed. No inertia: a defect has a velocity memory but no momentum, so inertia is a coarse property of clusters of field energy (Section 7). No strict bound: the speed has an edge, set by the rate of glides, that sits at c_0, with no γ factor below it, and a strict bound is not derived on L1. Defects reach the edge, a fraction at c_0 and none above (Table 3): a measured edge and no derived bound. **[Sim]** No lapse, no ruler and no static drive: a delay field with fixed stride and rulers is a scalar clock field, Nordström's theory [15], which bends no light; the second machine supplies the lapse and the ruler (Section 7). **[D]** The L1 reader of Section 5 finds the same nulls in its own clocks. **[Sim]**

7 The L2 machine: fluid, tension and frame layers

L1 and L2 are two scales of one reading. L1 is the routing substrate with no tunable parameter, at single bands and vertices; L2 works on the reader's chart cells, many L1 steps across, and keeps the transport that the topology of the Laves graph gives. Section 6 left four things out of L1 (Table 3): inertia, a strict bound, a lapse and a ruler. The lapse and the ruler are quantities of a chart link, its idle schedule and its number of fine passages, and inertia is field energy in a cluster; L1 contains none of the four. **[Sim]** L2 builds them on the chart scale, as the shapes of gravity and electromagnetism need; Section 8 runs it. L2 uses the network's own translation lattice, on the chart scale, with its two classes A and B; **[F]** it mirrors L1 further in one wave speed matched to c_0 and the defect density as the monopole source that L1-c reads with Gauss's strength (Section 5.4), and it is linked to L1 by the measured product of a hop rate and a cell given below. **[Rev]** It remains a model of mechanism, not a derivation from L1: its design choices are not derived from the principles, and each carries its grade, **[Rev]** with the physics it matches (Table 4).

Why the lapse lives here. The index of a gravitational reading splits into two halves, a space half, the ruler, and a time half, the clock, each the square root of the index; a purely spatial index gives light delay and no free fall. A round trip that visits a dwell site at distance r and returns has a weight proportional to $1/r^2$, ballistic or diffusive; a $1/r$ is a one-leg quantity, the Green's function of the floor, which in a time-invariant network is a constant lag, not a rate. A closure clock on L1 therefore reads no red $1/r$: the gravitational redshift is not an L1 clock effect, and the machine of this section places it by design. **[D]** Neither machine fixes a length or an energy in physical units: L1 has no intrinsic scale, and how a rest mass anchors to the floor is open (Section 9.2), so the experiments of L2 are scale-free tests of mechanism, which could sit far below the electron's scale or at a macroscopic one. **[D]**

Cells. The cells are those of the body-centred cubic lattice, bipartite truncated octahedra: class A at $\mathbb{Z}^3$ and class B at $\mathbb{Z}^3 + (\frac{1}{2}, \frac{1}{2}, \frac{1}{2})$, with eight hexagonal faces, each joining a cell to a cell of the other class, and six square faces, each joining a cell to one of its own class (Fig. 4a, b); Fig. 4c shows the packing. The class is a label only, and the content balanced. The transport cells are the reader's chart cells, not nested tiles of the Laves graph, which have no isotropic stencil of rank 4. Isotropy of rank 4 is a property of the stencil weights, $\sum_i w_i c_x^4 = 3 \sum_i w_i c_x^2 c_y^2$ for eight links of weight $1/18$ and six of weight $1/36$, chosen to match isotropic space; **[Rev]** the body-centred lattice is the network's own translation structure, the cube translations keeping the vertex class and t_{bc} exchanging it (Section 4, Appendix B.3), so its two classes are A and B, the same lattice on the chart scale; **[F]** it is also the lattice that D'Ariano and Perinotti find for the three-dimensional Weyl automaton [16]. The cell is a coarse-graining scale, asked only to span enough L1 steps that lattice detail no longer matters.

Three layers and one speed. Three layers share the cells (Fig. 5). The fluid layer is a lattice Boltzmann fluid on the links of the cells, with one relaxation rate for all stresses, which gives isotropy of rank 4 (the weights are in Appendix C.2). The tension layer is a rigid scalar ψ with the reversible second-order wave update at the speed c on the same stencil, and the density of defects as its monopole source. Its static solution is

$$\psi(r) = \frac{3s}{\pi V_2 \, r} \tag{8}$$

for a source of strength s (Appendix E.2), and the field moves with its source. The frame layer carries one U(1) phase on each link, with the temporal gauge and an exact discrete Gauss law, and charges are smooth densities (Appendix C.2). One speed c serves the tension and frame layers and the carrier of the clusters below. **[Rev]** The reason for the rigid layer is gravity: a diffusive carried mark gives the same static $1/r$ but lags a moving source by r^2/D, as in Laplace's argument on aberration, while a rigid layer updates at c and its field peaks at the source's present position. **[D]**

Gauss and Maxwell. The frame layer gives the Maxwell field of the machine, and Appendix E.3 assembles its four equations, Eq. (17). The discrete Gauss law is exact at every step, $G^T \mu A' = Q - \bar{Q}$, with A' the link potentials, μ the link weights and $\bar{Q}$ the mean charge, and a point charge has the Coulomb potential $q/(6\pi r)$, the weighted Laplacian satisfying $G^T \mu G = -6\,\Delta$ in graph units. **[D]** A charge in uniform motion carries its magnetic field, $\mathbf{B} = \mathbf{u} \times \mathbf{E}/c^2$. **[D]** A smooth density in uniform motion radiates only at the discretisation level, while a single-tick hop radiates. **[Sim]** Light has

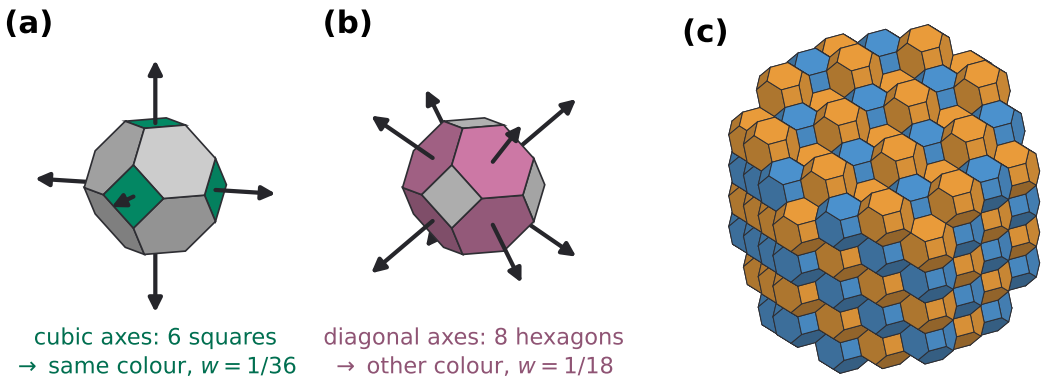


Figure 4: The cells of L2, truncated octahedra packed as the Voronoi cells of the body-centred cubic lattice. (a) One A cell, cubic axes: its 6 square faces lead to cells of the same class (weight $1/36$ each). (b) The same cell, diagonal axes: its 8 hexagonal faces lead to cells of the other class (weight $1/18$ each), and the rest weight is $7/18$. (c) A $4 \times 4 \times 4$ block of the packing as glass, A cells at $\mathbb{Z}^3$ and B cells at $\mathbb{Z}^3 + (\frac{1}{2}, \frac{1}{2}, \frac{1}{2})$.

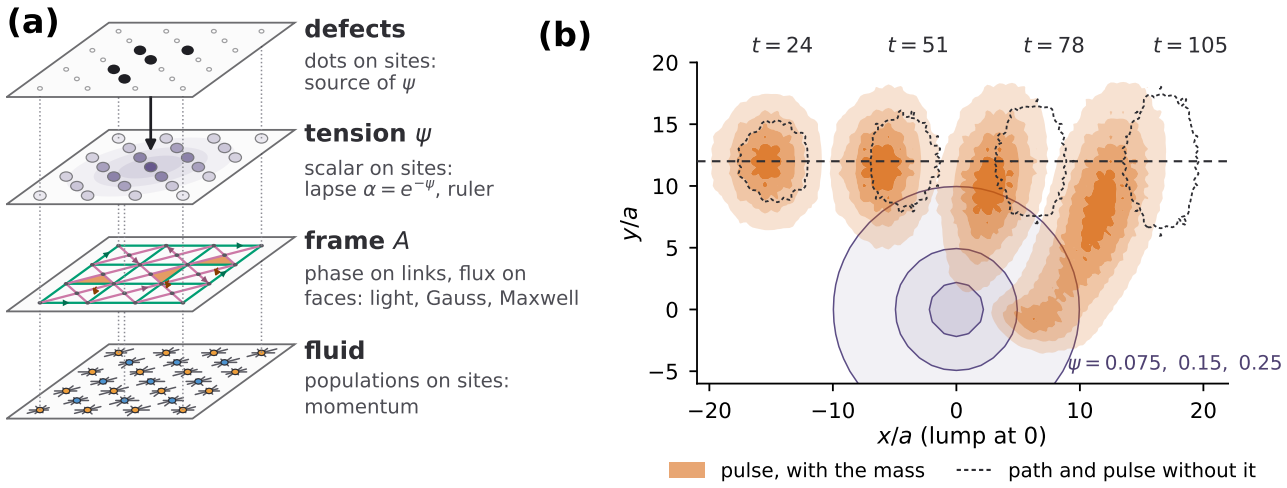


Figure 5: (a) The three layers of the L2 machine, and the defect layer that sources ψ, share one set of cells, shown in the [001] projection: defects source the tension ψ; ψ sets the lapse and the ruler; the frame layer carries a phase on each link and flux on each face; the fluid carries lattice-Boltzmann populations. (b) A frame-layer pulse passes a static ψ lump in the L2 engine, shown in the slice through the lump centre at four ticks t after emission; against the dashed straight path and the dashed outline of the same pulse in a flat medium, it lags and bends toward the mass. The lump is exaggerated for visibility ($A_0 = 1.5$, against 0.3 in the lens run), so the panel is a picture, not a measurement.

two isotropic polarisations and no birefringence when the square-link inertia is half the hexagonal one. **[Rev]** The machine gives the Gauss residual 2.7×10^{-14}, the Coulomb strength in units of $1/(6\pi)$ at 1.0003, and the isotropy of rank 4 of the potential to 2.5×10^{-4} with the box images removed (Appendix D.1). **[Sim]** The magnetic field of a moving charge is $|\mathbf{B}|c^2/|\mathbf{u} \times \mathbf{E}| = 1.04 \pm 0.05$, the radiation of smooth motion is a late energy slope of 3.4×10^{-5} against 0.042 for a hop, the birefringence is 1.8×10^{-6} and the spread of c^2 over directions is 4.6×10^{-11}. **[Sim]** The tension layer reproduces Eq. (8) to 0.99997 of its strength, isotropic to 2.3×10^{-4} with the box images removed, with the flux through a sphere at $r = 40$ equal to 1.0002 of the source. **[Sim]** The fluid conserves mass and momentum to 6.6×10^{-15} and 2.2×10^{-12}, its damping is isotropic to 4.4×10^{-5}, and with equal weights for the two kinds of link the isotropy fails, a spread of 0.56. **[Sim]**

Lapse and ruler. The lapse and the ruler are functions of the tension ψ:

$$\alpha = e^{-\psi}, \qquad \varrho = e^{\psi}, \qquad \alpha\varrho = 1. \tag{9}$$

The lapse α gates the hops and the clocks together by a deterministic idle schedule: transfers on each link take turns, losing parallel activity. The ruler ϱ is the number of fine passages per chart link, $n_l = \text{round}(N_0 e^{\psi})$, with N_0 the number at $\psi = 0$, and the product is one per link, from one conserved activation per link per tick on a schedule that no moving object can exploit to outrun the lapse; the lapse is a ratio of rates, and the ruler is written on the edges. The exponential form gives $\beta_{\text{PPN}} = 1$, where a linear law gives $1/2$. **[Rev]** Light's second factor of α is the ruler, matched to the impedance of the frame layer; putting the speed into one weight alone would reflect (Appendix E.2). **[Rev]** With them the delay of a ray through a region of tension (Appendix E.2) is

$$\Delta t = \frac{x_2 - x_1}{c}\left(e^{(1+\gamma_{\text{PPN}})\psi} - 1\right), \qquad \gamma_{\text{PPN}} = 1, \tag{10}$$

twice the clock-only value for small ψ, and the PPN parameters are $\gamma_{\text{PPN}} = \beta_{\text{PPN}} = 1$. **[Rev]** The measured values are in Section 8.

Design choice	Physics matched
stencil weights on the body-centred lattice	isotropy of rank 4
one speed c for every layer	a single limiting speed
exponential lapse $\alpha = e^{-\psi}$	$\beta_{\text{PPN}} = 1$
matched ruler, $\alpha\varrho = 1$	$\gamma_{\text{PPN}} = 1$, no reflection of light
$V_2 = 2$, $K_A = 1/2$	no birefringence of light, isotropic Coulomb field
cluster potential, sextic stabiliser	a stable lump of field energy

Table 4: The design choices of L2, all **[Rev]**.

Clusters as field lumps. A cluster is a gauged Q-ball: a complex carrier χ bound by a short-range scalar σ with a sextic stabiliser, all of its inertia field energy, with one speed c for χ, for σ and for the frame layer. **[Rev]** The binder σ is a minimal prototype closure, the least added structure that holds a charged lump together so that elastic scattering of massive, charged clusters can be run; any short-range binding would serve, and it is not the strong interaction and makes no claim about it. **[Rev]** Its static virial vanishes up to a discretisation residue, the von Laue closure, in which the binder compensates the electromagnetic stress. **[D]** In the static far-field test the tension layer is sourced by the lump's $T^{00} + \sum_i T^{ii}$, the Tolman source of general relativity, and not by the defect density of the dynamical layer; **[Rev]** given it, the far field is proportional to the total energy E of the lump, charged or neutral, because the von Laue virial vanishes, as the Tolman integral $\int (T^{00} + \sum_i T^{ii})\, d^3x = E$ requires (Appendix E.2). **[D]** The virial residue is 0.0058 of the lump energy and vanishes with the exponent 1.85 as the cell shrinks, the far field per unit energy of a charged lump over that of a neutral one is 0.997, the Tolman integral is 1.003 of E, and the Coulomb energy is 0.133 of the lump energy. **[Sim]** Inertia is field energy in a Q-ball. **[D]** Given the Tolman source, a closed static body's gravitating mass is its energy over c^2; clusters in the dynamical tension layer, as sources and in free fall, are not run (Section 9.2). **[Rev]**

The link to L1. L1 says what the network has at the defect level, a floor at c_0 and defects that diffuse and drift (Table 3); Table 4 lists the design choices of L2, each declared with the physics it matches. With the light speeds matched, $c\,a/T = c_0$ in L1 cells per L1 tick, L1 fixes only the product $a\,p_a = 3Dc/c_0 = 0.052$, from D and c_0 above with $c = \sqrt{2/3}$, with a the L2 cell in L1 cells, p_a the hop probability of the defects on L2 and D the diffusion constant of Section 6. **[Rev]** The runs take $p_a = 3Dc^2/(c_0^2 T)$ with $T = 1$ L1 tick per L2 tick, a declared choice that sets only the diffusive equilibration time of the sedimentation run (taken literally at $T = 1$ it would give $a < 1$); the equilibrium $n \propto e^{\psi}$ does not depend on it, and no result of this paper depends on that choice of T. **[Rev]**

8 Toy-universe experiments on L2

Each experiment here is a run of the machine of Section 7, read by closures: readers that count arrivals in their own ordinal, as in Section 5. The expectation is stated first, as a formula of the model, and the run gives a value with its error. No experiment is an analogy: each is a reading of a toy universe built from the layers, whose laws are its own. Every machine number is a key of the L2 readouts, listed in the record's README by the rows of Table 6 (Appendix D.2), and every run is **[Sim]**. Some runs check that the code obeys a declared rule (event clocks read the lapse, sedimentation, $\gamma_{\text{PPN}} = 1$ with the matched ruler); the others are experiments whose outcome the design does not fix (scattering, delayed choice with a physical analyser, the slab reflection control).

8.1 Gravity

Static and moving fields. A point mass has the tension $\psi \propto 1/r$ of Eq. (8). A moving mass is read by the Heaviside field of Eq. (7), centred on the present position of the source; the tension layer tests it with a source in uniform motion. The peak sits at offsets of 0, -2 and $+1$ cells from the present position at three distances. **[Sim]**

Lensing and Shapiro delay, read by closures. For a ray at impact parameter b past a mass of far-field amplitude A_0, the matched medium of Eq. (10) gives the deflection and the delay

$$\kappa = \frac{2(1+\gamma_{\mathrm{PPN}})A_0}{b}, \qquad \frac{d(\Delta t)}{d\ln b} = -\frac{2(1+\gamma_{\mathrm{PPN}})A_0}{c}, \tag{11}$$

with $\gamma_{\mathrm{PPN}} = 1$ from the matched ruler of Section 7, a check of the declared rule: general relativity's value, which doubles the deflection and the delay of a lapse alone ($\gamma_{\mathrm{PPN}} = 0$; the weak-field static metric, Appendix E.3). **[Rev]** Eq. (11) holds for paths much longer than b and the run's are not, so closure readers are compared with the same $\gamma_{\mathrm{PPN}} = 1$ medium, ray-traced through the run's own ψ with the lattice's dispersion. On the rows where geometric optics holds, impact parameters of at least 4.2 Einstein radii, the deflection lies 0.024 and 0.026 above the traced value at the two resolutions, full and conv (Appendix D.1), against the tolerance 0.021 set by the omitted wave term: an honest miss, the same at both resolutions and not explained; the delay along that ray is 0.978 and 0.993 of the finite-path eikonal (tolerance 0.045). The slab reads $\gamma_{\mathrm{PPN}} = 1.004$ and 1.002 (tolerance 0.008), against 0.010 for the control with the lapse alone. **[Sim]** Through a slab the delay of the full medium is 2.101 times the clock-only delay, against 2.096 for the exact slab profile, and the matched medium reflects 3.6×10^{-10}, against 0.0022 with the ruler left out. **[Sim]**

Clocks. Event clocks, which count lapse-gated events, read the lapse, $\omega = \omega_0\,\alpha_{\mathrm{s}}/\alpha_{\mathrm{r}}$, so the redshift of an event clock is the ratio of the lapses of source and reader, a check of the declared gating. **[D]** The event clocks deviate from $\alpha_{\mathrm{s}}/\alpha_{\mathrm{r}}$ by 2.4×10^{-5}; a cavity clock of fixed chart size, a fixed link count, reads the lapse squared, its frequency ratio deviating from $e^{-2\langle\psi\rangle}$ by 0.0020 and from $e^{-\langle\psi\rangle}$ by 0.036. **[Sim]** A cavity of fixed proper length would read α, since $\alpha\varrho = 1$, and is not built. **[D]** Whether bound matter keeps its chart size or its proper size is open (Section 9.2).

Sedimentation. Hops gated by the lapse at the departure site, a design choice of Section 7, give a stationary density $n \propto e^{\psi}$: gravity has the right sign, as an equilibrium profile and not as free fall. **[Rev]** The slope of $\ln n$ against ψ is 1.00000, with mass conserved to 2.1×10^{-12}. **[Sim]** The hop rate p_a (Section 7) sets only the time to this equilibrium.

8.2 Charge and light

Two charges of the same sign repel at the Coulomb energy $q_{\mathrm{s}}q_{\mathrm{r}}/(6\pi r)$ and opposite charges attract, by the Maxwell equations of the frame layer with positive field energy, and light is the radiation part of the frame layer, with two polarisations that no medium of the machine splits (Section 7). **[D]** The machine gives the sign $+1$ for like and -1 for opposite charges. **[Sim]** A reader reads a charge through the composed product of Section 5, and its quantum is the number of carrier quanta of a cluster, a continuous Noether charge on L2 and an integer only as a coarse property (Section 9.2). **[D]**

8.3 Interference, markers and the eraser

The experiments here read the wave; the counting statistics are discussed in Section 9.1.

Double slit. Two equal slits, a distance d apart, give fringes of spacing $\lambda L_{\mathrm{s}}/d$ at a screen at distance L_{s}, with full visibility, since the wave equation of the layers is linear. **[D]** For the polarisation Z, the electric field along the slits, at screens 54, 80 and 108 cells from the slits, the machine gives the visibility 0.965 to 0.988, the spacing against the exact two-source pattern 1.002, 1.001 and 1.002, the local coherence 0.92 to 0.98 and a deviation from linear superposition of 0.015 to 0.031. **[Sim]** In the far field, at 160, 216 and 296 cells, the spacing in units of $\lambda L_{\mathrm{s}}/d$ is 0.991, 0.988 and 0.996, and against the exact two-source phase slope 0.9905, 0.9886 and 0.9947; the 160-cell value against the two-source slope misses its tolerance of 0.52%, lying 0.77% low after Richardson extrapolation of the resolution pair, a geometric offset that shrinks with L_{s}, not a resolution error (Appendix D.2). **[Sim]**

The in-plane polarisation Y, the electric field across the slit width, reads 0.965, 0.961 and 0.963 in the same units, 3.5 to 3.9% low; it is reported as measured, since the two-source prediction carries no polarisation and the slit–slit coupling through the clamped wall is not traced. **[Sim]**

Markers and the eraser. A which-path marker of strength τ, the root of the ratio of the marked to the clean energy, lowers the coherent visibility, monotonically in τ, and a marker switched on after the pulse has passed acts as none: causality. **[D]** The coherent visibility is 0.839 and 0.492 for two marker strengths, falls monotonically in the delayed marker's strength τ_2, and a late marker differs from none by 1.9×10^{-4}. **[Sim]** With a which-path tag of orthogonal polarisations on the two slits, the fringes of the total intensity vanish, and the projections on $+45^\circ$ and -45° restore fringes and anti-fringes, whose sum is flat. **[D]** The tagged total has visibility 0.0085, the $+45^\circ$ projection 0.938, the phase difference of the two projections is 0.9996 of π, and their sum is flat to 3.1×10^{-16}. **[Sim]**

Delayed choice. An analyser switched on after the pulse has passed the slits gives the same fringes as one in place from the start, since the reading is made by the reader's projection and not by the layer. **[D]** The late analyser differs from the early one by 5.0×10^{-4}, and a physical analyser layer on from the start differs from the reader-side projection by 0.074, with visibility 0.948. **[Sim]**

The background as dephasing. A uniform background changes nothing for lapse-gated clocks, since the lapse rescales all clocks alike, and a stochastic background dephases by random shifts of the relative phase of the two paths, without a which-path record: the local coherence stays, the visibility of the ensemble falls. **[D]** The strength of the stochastic background is a parameter of these runs, since L1 does not fix the global background offset it needs. A uniform background leaves the visibility at 1.0001 of its value and the spacing in proper length at 0.9987; the stochastic background shifts the fringes by 0.288 turns rms, the visibility of the ensemble is 0.551 of the mean visibility, and the local coherence stays at 0.954. **[Sim]**

8.4 Scattering of clusters

Two like-charged clusters of Section 7, aimed at impact parameter b with a relative speed v, repel at the Coulomb energy $q_1q_2/(6\pi r)$, and at low speed their orbit is Rutherford's: the centre-of-mass deflection obeys

$$\tan\frac{\theta}{2}=\frac{q_1q_2}{6\pi\, b\,\mu v^2}, \tag{12}$$

with μ the reduced mass. **[D]** At $b=40$ cells and $\gamma\beta=0.35$ the clusters separate intact, the lab deflection in free space is -33.7° against -35.0° for the point-charge orbit, the momentum balance is 0.0025, the energy drift 3.0×10^{-4} and the carrier number kept to 0.994. **[Sim]** Near the speed of light, at $\gamma\beta=0.75$, the deflection in free space is -10.9° against -11.9°, with momentum balance 0.022 and energy drift 0.0011. **[Sim]** The deflections are shown against the point-charge orbit and are not graded: no tolerance was declared for them. At an impact parameter of 20 cells and $\gamma\beta=0.75$ the clusters touch, with closest approach 0 cells, outcome fused and energy kept to 0.0011; contact is governed by the attraction of the binder, and the repulsion at contact is left open (Section 9.2). **[Sim]**

The Lorentz law and the strict bound. A lump boosted to $\gamma\beta$ has the energy $E=\gamma Mc^2$ with $M=E_0/c^2$, E_0 the rest energy, the momentum $P=Ev/c^2$ and a contraction $1/\gamma$ along its motion, insofar as the sudden kick does not radiate. **[D]** At $\gamma\beta=1$ the energy ratio $E/\gamma Mc^2$ is 1.026, the momentum ratio Pc^2/Ev is 0.981, the contraction ratio is 1.12, shown and not graded since no tolerance was declared for it, and the kick radiates the share 0.095. **[Sim]** In the runs no signal and no lump moves faster than c: the bound is measured, not derived. **[Sim]** Under a constant force the largest speed over a window is 0.657 of c, 0.928 of the Lorentz value, the energy follows γMc^2 to 0.984, and the velocity follows Pc^2/E to 0.913. **[Sim]**

9 Discussion and open problems

Sections 5–8 carry the measured claims; this section sorts the rest: the discussion holds what is argued in shape, each item with its grade, but has no machine, the open problems what is not yet known in shape.

9.1 Discussion

Stretch of a sky: trace and traceless. The stretch of a reader's sky, in the Möbius map of Section 5, has a part common to every direction and a part that picks out an axis. The trace part, one number for all arrivals of one reader, is read as the cosmological redshift, a drift of the reader's tick length, and the traceless part, which has the form of a dipole about an axis $\hat{u}$, is read as motion. **[L]** What distinguishes them is symmetry alone: an isotropic drift cannot make an axis, and a compact rotation of the sky cannot compose into either. **[D]**

Friedmann from the drift. No reader reads the network tick n; the readout cosmology identifies it, by choice, with conformal time η, which the uniform floor allows, and the only conversion that drifts is the reader tick length b in network ticks. A reader cell holds b^3 network cells, so its held content dilutes as b^3. Read through the Friedmann equation of general relativity, in the continuum limit b obeys

$$\left(\frac{db}{d\eta}\right)^2 = \mathcal{C}_\Lambda + \mathcal{C}_\mathsf{m}\, b^3, \qquad H = -\frac{db}{d\eta}, \tag{13}$$

in which Λ is only a first integral, as in unimodular gravity [17, 18, 19]. **[Rev]** The vacuum, the floor's readout name, has a held level, its held content per reader cell, which enters $\mathcal{C}_\Lambda$ as a share in reader units; per network cell it would dilute as b^3 and be matter. **[Conj]** Given Eq. (13), the scale factor $1/b$ increases and is convex in conformal time in every era (Appendix E.4), so it never saturates, and the bounded, saturating mixed fraction of the floor cannot be it. **[D]**

Flatness. The Laves graph is the maximal abelian cover of K_4 (Appendix A.3), so the network is combinatorially flat: its growth is r^3, and a negative curvature would need exponential growth and a positive one a closed sphere. **[D]** Eq. (13) then has $k = 0$, an input, so there is no flatness problem and no inflation is needed for it, and $\Omega_k = 0$ globally, consistent with $\Omega_k = 0.0007 \pm 0.0019$ from Planck with baryon acoustic oscillations [20]; global $k = 0$ in the readings also needs a uniform drift b of the reader cell. **[Conj]**

The reader-side screen. A second route to the same equation goes through an area bound on a horizon and the Clausius relation on it [21]. If Newton's constant is a number times a cell area, that cell is a reader-side screen cell of fixed area in reader units, since a network cell would give $d \ln G_\mathsf{N}/dt = 2H$, beyond observed bounds. **[Conj]** The holographic screen then sits on the reader's side, not on the network. **[Conj]**

The end state. The state space is finite and the rules deterministic, so every history is eventually periodic: network time is a transient and a circle, and the unbounded ordinal is a label of the frame. **[D]** In the continuum limit the Λ era ends with b falling linearly to zero at a finite η_∞, and $H_\Lambda^{-1} = (\eta_\infty - \eta)/b$ stays constant; on the finite machine the divergence in reader time is cut off at an absurdly large but finite value. **[Conj]** The end state is therefore cyclic as structure and eternal as read: the recurrence returns every memory with the state and is not readable from inside, and a reader that falls into degeneracy is no longer a reader, so no closure outlasts it to read the cycle. **[Conj]** The knee $H^2 = 2H_\Lambda^2$, where the held content of a reader cell falls to the held level, is by definition the matter–Λ equality. **[L]**

The quantum character. The layers are linear, so interference, which-path markers, the eraser and delayed choice are wave phenomena of the field; what is quantum is the reading by counting. A counting reader sees two kinds of statistics (Appendix E.4). Counts of independent arrivals, a product state in local equilibrium, are Poisson at their intensity by the limit of rare events, and single registers are binomial, $g^{(2)}(0) = 1 - 1/M$ for M of them, down to $g^{(2)}(0) = 0$ for one register, since it holds one bit. **[D]** The collective mode, a nearly Gaussian sum of many modes, is thermal-like, $g^{(2)}(0) = 1+1/M$. **[D]** A count in a resolution cell of M modes that receives both has Var $n = \bar{n}+\bar{n}^2/M$, the particle term from the counts and the wave term from the collective mode. **[D]** Which side shows is set by the regime, clicks for $\bar{n} \ll 1$ and fringes for $\bar{n} \gg 1$, and by the reader's form: linear readers read the wave and counting readers read counts. **[D]** Statistics belong to the channel, not to the object. **[L]**

Bell correlations at readout. A walk-sum path leads from the $\lambda = \frac{1}{2}$ channel to the correlation $-V\cos\theta$ and Tsirelson's value $2\sqrt{2}\,V$ at the readout layer, where Fine's result lets readings that resolve one pair event exceed the CHSH bound when the pair coherence V exceeds $1/\sqrt{2}$ (Appendix E.5). **[Conj]** The routing network is local and deterministic. **[F]** "Outside the system" is not defined, since the system is a mathematical structure and physics is the readout layer, so a chooser of settings independent of the pair, which measurement independence presupposes (its relaxation is studied formally in [22]), has no meaning here and is not assumed, so the network's locality holds, and if the walk-sum path above holds, the readout's excess over the CHSH bound can hold with it. No machine runs the path (Section 9.2).

9.2 Open problems

Each problem says what is missing.

- *Clock universality.* Event clocks read the lapse α and a cavity clock of fixed chart size α^2, while a cavity of fixed proper length would read α (Section 8), and one redshift needs one of them: whether bound matter keeps its chart size or its proper size is missing.
- *Gravity of moving bodies.* The tension layer of L2 is scalar, with the source $\gamma M(1+\beta^2)$ against the trace M/γ of a moving lump; the far field of a moving body is not yet measured, and the Tolman closure holds for closed static bodies only.
- *Spin 2.* The gravity of L2 is the scalar ψ, and no tensor mode exists in it.
- *Nonlinear gravity.* $\beta_{\mathrm{PPN}} = 1$ is declared by the exponential law and untested, and the nonlinear field equations of general relativity are not reached (Appendix E.3).
- *Strong field and horizons.* The exponential lapse never vanishes for finite ψ, and Finiteness bounds the held density, so there is no metric horizon and no singularity, and here the theory parts from general relativity. A horizon here would be one of readout, where the lapse sinks a source's signal below a reader's resolution, the floor's fluctuation $0.5/\sqrt{N_{\mathrm{eff}}}$ of Section 5.3. Not run.
- *The origin of σ and the quantisation of charge at L2.* The binder σ and the sextic stabiliser are design choices of Table 4, and the charge of a cluster is a continuous Noether charge; the integer class charge of L1 and the coarse integer of L2 have not been joined.
- *Contact repulsion.* At an impact parameter of 20 cells clusters touch (Section 8.4); a repulsion at contact is absent from the machine.
- *Chirality of the weak interaction and the particle content.* Chirality, the particle scales, the generations and the held level lie outside the machines of this paper, and rest also on the primordial pattern; how a rest mass anchors to the floor is open too.
- *Moving readers.* The integral of a moving reader's frequency shift against the change of the static potential is derived along a prescribed trajectory (Section 5); what is missing is a machine

measurement of the network form of the equivalence principle: that holding delays the causal flow alike for readers of every kind, up to the conversion of scale.

- *The two routes to Friedmann.* Whether the Clausius route with a reader-side screen returns the drift equation and its first integral is missing.
- *Clusters in the tension layer.* The dynamical tension layer is sourced by the defect density only; clusters as sources in it, and their free fall, are not run.
- *Bell correlations.* L1 has no walk-sum engine, so the pair coherence V is not measured; no source closure is shown to write a weight-0 modulation onto two flows with correlated sheets; no reader closure is shown to resolve single pair events; and that machine counts with late settings follow $-V\cos\theta$ is not shown (Appendix E.5).
- *The torus zero mode.* On T^3 the rigid layer's zero mode is driven by the net source and is a uniform drift of $\ln\bar{n}$ under the reader's conversion; a global neutraliser in it would be a term of the cosmological-constant kind, and whether the amplitude of the floor's noise can enter a dimensionless mass ratio, against the bounds on a drift of the proton-to-electron mass ratio, is not known; the periodic layer is not run.
- *Reading the dispersion.* Whether a reader whose window nears the coarse-graining scale, about seven cells, could read the dispersion of the collective mode and its anisotropy is not shown; it mixes a distance on the network with a count on the reader's side.
- *The lattice orientation.* Whether an extended reader's rotation could make the orientation of the lattice readable is missing.

10 Conclusion

This paper builds one causal network on a fixed graph, a purely mathematical structure, and studies what it can be read as, in two steps. The first is a routing machine on the Laves graph of a three-torus, whose routing, swap and hold rules have no tunable parameter and whose step decision has declared choices. Readers inside it receive only counts of the flow, and under declared conventions the counts read as rest mass, charge and motion, with relativity entering at readout on L1 and by design on L2, as the relation of dynamics and frame of Section 5. Moving defects, the transport they hand up and the nulls they leave (Section 6) show what the routing machine does not contain: inertia, a strict bound, a lapse and a ruler. The second step is a coarse machine of three layers, a fluid, a tension and a frame layer, whose design choices are declared and graded (Section 7), and whose toy-universe experiments give lensing, clocks, interference and scattering, each with its measured value (Section 8). Appendix E.3 assembles Maxwell's equations, and the weak-field static Einstein equations only, and says what is not reached. Every claim carries its grade; the code, its tests and the hashed run records are released, and Section 9 names what stays open. Appendices A and B record how the principles motivate the graph and how the lock writes its bands; they supplement the construction and do not carry the paper's central claim.

Sources of inspiration. Pieces known from separate fields reappear here as rules or readings of one construction, and the paper owes them its direction. The principles take distinction as the primitive act, as in Spencer-Brown's calculus of indications [23]; before the lock the rules are deterministic and reversible, as in the automata proposed beneath physics [24, 25], and an unhold forgets its entry band, the erasure at the root of irreversibility [26]. Coarse-grained, as in hydrodynamic limits [27], the flow carries the sound mode of lattice gases [13, 14], and the defects among fixed scatterers form a gas as in the Lorentz gas [28, 29]. On the reader's side, Bondi's radar account [8] returns in the Doppler factor, and the window law rests on Kac's recurrence [12]; and Λ is read as an integration constant of the Friedmann equation [17, 18, 19]. A further source is twistor theory [30]: twistor space has no time of its own, spacetime points and fields are read out of it through an integral transform, and

motion is a product of the transform; the paper puts causal flow where twistor theory has light rays, and reads it out by an integral transform, the incidence transform, of which the Penrose transform is the holomorphic version.

The construction joins the programs that look beneath spacetime geometry: pregeometry [31, 32], spin networks [33], causal sets [34], digital physics [1, 2], hypergraph rewriting [35] and quantum graphity [36]. What it adds is a fixed graph, on which no rule adds or removes a vertex or an edge; two machines whose readings can be run and graded; and relativity entering at readout, with c_0 as the conversion ratio between space and time, from which the Lorentz transformation follows. Two neighbours differ in what they fix: in causal dynamical triangulations the extended dimensions are produced by the dynamics of a sum over geometries [37], whereas here the three dimensions are read from the translations of the graph the principles select, and Lorentz invariance is a reading under the relativity convention. Quantum cellular automata reach Weyl, Dirac and Maxwell dynamics with approximate Lorentz covariance [16, 38]; this construction differs in its fixed graph, its lock and its readout channels, and the two are not ranked here. Because every one of these is a rule or a reading of one construction, the pieces hold together in one mathematical frame whose consistency can be run: this integration is the paper's significance.

A Principles and the construction of T^3

A.1 Principles

This subsection fixes the principles' working form, to which the grades **[F]** and **[D]** refer; it supports the motivation of the network (Section 2), the venue rule (Section 3), and no pair creation and the two-tick move (Section 6). Finiteness refuses infinity, so compactness is forced and the number of bits sealed. Distinguishability admits only what can be distinguished, and drives the construction while a local rule can still unlock a readable distinction. Minimal sufficiency adds only rules that unlock new readable content, a distinction no local rule could read before; it drives nothing and cuts rules, not implementations. Relationalism, read as the relativity principle, admits only what a reader reads from relations, never a network tick or place (Section 5.1). These premises carry no grade; they are taken, not provable inside the theory.

Finiteness seals inflow only: nothing enters from outside, erasure of relations, a path or a timing, is allowed, never of types, and compactness orders no events. Distinguishability takes two steps, a mark against no mark, then the mark's two sides defining each other, so which value is named 1 is a gauge; before the lock no rule tells the values apart, so rules commute with X (Section 4), and the occupancy $1/2$, this symmetry read, persists, as a later stage does not dismantle an earlier category. In working form it is a count statement: no event changes the count of either value on either strand, and the types are the value and the strand χ. The lock names the values by the handedness of its half twists, one undetermined bit chosen before the lock. The symbol 1 has three layers: a gauge of the network; a rule, the hold, which is asymmetric in 0 and 1 and so defines the stoppable kind without reference to the symbol, rest mass being its held count; **[L]** and a reader's, energy being $\overline{h}$ times a count times the clock, never the number of 1s.

The lock unlocks a contrast between vertices, so by the drive the irreversible cut runs between vertices and events live on venues. **[D]** On a band this is forced: crossing an untwisted band as if untwisted is the identity. **[F]** At a vertex it follows from the cut: a vertex not overtwisted hosts no event. **[D]**

The network stores no coordinate, since a position label would enter from outside and no rule reads an ambient manifold; no shared clock, since a free choice would enter from outside and a second writer would make outcomes depend on update order, hence one writer per register and confluent rules; and no field, since a register holds one unnamed binary distinction, so before the lock the state is occupancy alone. **[F]**

Every event keeps the count of each value on each strand, so the number density N and the strand difference Q are conserved. **[D]** Class charge, $q_{\mathrm{cl}} = n_A - n_B$ over the defects, is exact at every tick, and the defect number is constant, since inside a glide the stray stops on w and v' make no seat; free pair creation is left out, since a propagating carrier needs a nearly defect-free floor. **[Rev]** The hold keeps both strand counts and delays, but the delay is not forced: of the maps on six entry registers per vertex, one that is C_3-covariant, keeps both strand counts and needs no delay has an image of 61 of 64 states, so the buffer is chosen, to read as rest mass held as delay. **[Rev]** The class charge makes a defect's move last more than one tick: if stops move at most one bond per tick and every stop sits in a full vertex triple at the start of the tick, a tick that moves a defect changes q_{cl} or the defect number n_{def}, checked exhaustively on a ball of the universal cover (a cubic tree, every defect set within depth two), on $K_{3,3}$ and on the cube graph. **[F]** The premise matters: with stray stops a defect moves from one A vertex to another, at distance 2, in one tick and keeps both. **[F]** The glide of Section 6 meets the premise, since it starts only from rest and its intermediate state is the only place with stray stops. **[D]**

A.2 Lemmas on local maps

This subsection holds the four lemmas that Appendix A.3 uses to fix the degree of the network. A local map is restricted by Distinguishability twice: before the lock it commutes with X, since no rule tells the values apart, and it reads every input, an unread input being gauge. **[D]** *Two-input lemma*: a map from two input to two output registers that commutes with X and reads both inputs is a bijection, one of eight that pass or cross the bits, each with one of four bitwise complements. **[F]** *No-merge lemma*: none of the eight reads its inputs jointly, merges two inputs or writes an output from none. **[F]** *Three-input lemma*: of the eight maps on three registers that also commute with every permutation of the bands, four are not injective: majority or parity on every output, and their complements. **[F]** *Routing lemma*: routing read from the bands moves each bit along a curve with one successor at each point, so it permutes the registers for any twists and overtwisted vertices. **[F]** The open premises are one register per input, where the machine has six entry registers per vertex (Appendix C), and one reader per register.

A.3 Construction of the three-torus

This subsection supports Section 2: the principles build a zipper of degree three on a circle, and the steps below select the Laves graph on a three-torus. A distinction has one successor and one predecessor, a bijection on a finite set and a single cycle if connected; a segment's ends would have degree one, against one rule everywhere, so the first object is a circle. **[F]** Its second side, fixed by the first since inflow is sealed and differing from it for both values, is its complement, so every mirror pair holds one 1 and no distinction is added. **[F]** By the no-merge lemma this two-way circle unlocks nothing, so the drive adds the least structure giving every vertex three inputs, one chord per mark, an edge joining two marks that closes the circle like a zipper, and degree three is the first at which a rule can read content (three-input lemma). **[F]** A cyclic order chosen vertex by vertex would let one bit per vertex in, a bit that no local rule could read before the lock, so Minimal sufficiency cuts it and one rotation system holds everywhere. **[D]** Finiteness excludes the tree, since a finite graph with every degree at least two has a cycle, and cycles are what closures need. **[F]** Distinguishability excludes a quotient with parallel edges, which would need an identity the relation does not ground, so the quotient is a simple cubic graph, with $V_0 \geq 4$ vertices. **[D]** Degree three gives three families of straight routes, and the drive adds structure until they are three distinguishable directions; on four vertices they already are, so Minimal sufficiency stops there, since a larger quotient adds directions that no family needs. **[D]** The simple cubic graph on four vertices is K_4, with $b_1 = 3$. **[F]** Two walks with the same net count on every edge end at the same vertex: a second vertex with the same counts would need an identity that no count grounds, which Distinguishability excludes, as it excludes parallel

edges. **[D]** Concretely, the commutator of two face loops of K_4 that share an edge reduces to ten steps and closes on the cover; these are the ten-rings, fifteen through each vertex, and no shorter walk of zero count exists in K_4. **[F]** So the network is a quotient of the maximal abelian cover of K_4, the Laves graph, by translations, and its ten-rings are the cycles that lift open (Section 5.1). **[D]** Among three-periodic nets only the diamond, of degree four, and the Laves graph have maximal symmetry and strong isotropy [7]: here strong isotropy is a property of the graph selected, not a criterion for selecting it. **[F]** The three-torus is the finite, unbounded and minimal quotient by translations alone: a quotient with a rotation would permute the route families around a cycle and unlocks no readable content, which Minimal sufficiency cuts. **[D]**

A.4 Direction and isotropy

This subsection derives what Section 2 states about the directions of the network. A direction is a class in $H_1(K_4;\mathbb{Z}) = \mathbb{Z}^3$, a deck transformation of the Laves graph, the maximal abelian cover of K_4: how the structure maps to itself, with no embedding, of rank $3 = b_1(K_4) = 6 - 4 + 1$. **[F]** The group $\mathrm{Aut}(K_4) = S_4$ lifts to the cover and acts irreducibly on $H_1(K_4;\mathbb{R}) = \mathbb{R}^3$, as the rotations of the cube, so by Schur's lemma every invariant quadratic form on directions is a multiple of the identity. **[D]** The coarse metric is the covariance of the walk on the cover [7], isotropic without orthogonality or an embedding: the inner product is produced by the dynamics, not assumed. **[D]** Its reading as flat space is in Section 9.1 (Flatness).

A.5 Where irreversibility sits

This subsection supports Section 3 in five steps, using no machine rule. Irreversible events exist: halting while a local rule can still unlock an arrow violates the drive of Distinguishability. **[D]** The lock leaves overtwisted vertices: writing only a uniform twist is injective, and a distinction between dwelling and passing needs both sides non-empty. **[F]** No renaming of sides removes the lock's half twist on every band, so every band is a venue for the swap, its own inverse, and holds on bands are excluded, since the irreversible cut runs between vertices. **[D]** Plain vertices host no event and only route, which permutes the registers. **[D]** Every update off overtwisted vertices is thus a bijection, and irreversible events and held states sit only at overtwisted vertices. **[D]** Whether that event is a hold is the machine's choice (Appendix C); the open premises are the lemmas' (Appendix A.2).

B Band topology and the lock

None of this appendix's results assumes a particular pattern of overtwisted vertices.

B.1 Bands and the lock

This subsection supports the routes, the venue rule, the mixing and the missing J_{hist} (Sections 2, 3) and the total framing (Section 6).

Sides and routes. Before the lock a band's two strands are its sides: an untwisted band keeps each bit's side, and a full strand beside an empty one could not mix under rules that conserve both strand counts. **[F]** Counts are conserved side by side before the lock and strand by strand after it, and only the occupancy $1/2$ carries across to χ. **[F]** A half twist crosses a band's sides once and so reconnects the routes: with every band twisted the turns alternate and routes run straight as Petrie walks, so the uniform twist is Petrie duality [39]. **[F]** Its walks are the routes of untwisted bands with every B vertex, or every A vertex, overtwisted, related cycle by cycle by $s \oplus [u \in \mathrm{B}]$, so writing on the bands picks no class. **[F]** A face loop uses each band family once per period and three of the four families meet at each vertex; after the lock each vertex lies on one helix of each axis family; on the

machine's realisation the face loops are right-handed and the axis helices left-handed. **[F]** No route of either phase is contractible on the torus, and both phases span a lattice of rank 3. **[F]**

Framing. At the isotopy layer, with straight bands and flat vertex discs, a contractible cycle's framing is its base value plus half the sum of τ_e over its bands, and on a theta graph of two ten-rings sharing the band e, closed by a contractible eighteen-ring (Fig. 6c), the framings obey $\mathrm{Fr}_1 + \mathrm{Fr}_2 - \mathrm{Fr}_3 = \tau_e$. **[F]** At the homotopy layer only the framing mod 2 survives, one $\mathbb{Z}_2$ flux per ten-ring. **[F]** The identity $\sum_e \tau_e = E + N_{\mathsf{stop}}$ holds by declaration (Section 6), so the total framing is constant except inside a glide, where it changes by $+4$ and then -4. **[F]** The framing is t_{bc}-even and J_{state}-even, and even under reflection when counted relative to the lock's handedness. **[F]** A pinch, the two sides of one band passing through each other, takes τ_e from 1 to -1 and is the least event that changes the band embedding and conserves no framing. **[F]**

The lock. Any half twist makes a band a venue: a venue rule that reads only whether a band is twisted draws one distinction fewer than one that reads the parity of its twist count (Minimal sufficiency, Appendix A.1), and counting only odd numbers of half twists would bar swaps on bands with one overtwisted end. **[D]** Twists written between ticks never mix: an untwisted band keeps the sides, and a twisted one then holds a side of 1s against a side of 0s, so its swap changes nothing and no seat can hold a pair; the side-ordered start is a fixed point under any history of twists, defects included, and either labelling of content. **[F]** Routing sees a new twist in the tick it is written and swap detection, which runs first, a tick later, so each band's first twisted crossing is unprotected. **[F]** Routing reads $g_e = \tau_e + \mathrm{rot}_u + \mathrm{rot}_{u'} \bmod 2$ for band e with ends u, u', rot_u the rotation-system bit of u, so one more half twist on a vertex's bands reverses its turning and leaves routing unchanged, and holds read f_u (Appendix C). **[F]** A lock rule that reads only the handedness cannot write a t_{bc}-odd integer, because t_{bc} is a translation and keeps the handedness; whether such a rule must read the product of handedness and class at a vertex is untested. **[F]** Of the sixteen occupancies of a band's four entry registers, exactly two give different outcomes with and without the twist while changing no strand count, and there the swap fires. **[F]**

Mixing and pasts. The offsets of the net and of its mirror under the exact $\mathrm{Mir} \circ t_{\mathsf{bc}}$ differ by $(-0.2 \pm 2.2) \times 10^{-5}$, and with overtwisted vertices written on their bands the flow behind the lock's front mixes at them too, as Section 3 measures. **[Sim]** With no overtwisted vertex, a twist written everywhere at once complements every register's side order, and nothing mixes. **[F]** A seat's update merges states, so a held state has several pasts: at an isolated overtwisted A or B vertex with the rest of the flow empty, the 256 states of its six entry registers and its buffer have 211 successors. **[F]**

B.2 Frames and the spin lift

This subsection supports Section 5: the double cover of the register frames and the Hopf map. The register frames of the network form the octahedral group O of order 24, one free orbit of it, and their lifts form the binary octahedral group $2O$ of order 48, a nonsplit central extension of O by $\mathbb{Z}_2$ whose only involution is -1. The sheet exchange is central, and the lift of the exact fourfold rotation has fourth power -1, so a 2π rotation built from an exact symmetry acts as -1 on $\lambda = 1/2$. **[F]** The Hopf map sends the 48 lifts onto the 12 arrival directions, four over each, a discrete fibre $\mathbb{Z}_4$. **[F]**

B.3 Discrete symmetries

This subsection proves Section 4: exactness and its parity law, the orbit of handedness and class, the sign ledger.

Exactness. At the seats t_{bc}, Rot_4, Rot_2, Mir and X each break alone, as do the four products with X that were run and $\mathrm{Mir} \circ t_{\mathrm{bc}} \circ \mathrm{Rot}_4$. Checked on a 3-cell torus, the named exact operations pass and each named broken one fails a table, and each of the 48 exact operations, one per coset below, maps the tables of the glide (Section 6), the step table, both ticks' stop sets, the contact shell and the floor momentum to themselves. **[F]** For every proper isometry g exactly one of g and $\mathrm{Mir} \circ g$ is exact with holds: $\mathrm{Mir} \circ g$ if and only if g either exchanges the classes or permutes the cube axes oddly, but not both, where fourfold rotations and twofold rotations about face diagonals are odd and the rest even. **[F]** On a 12-cell torus the 82 944 such operations form 48 cosets of the exact, class-keeping primitive translations and 23 geometric classes, and every coset and class obeys the law, which extends the parity of the turning (Appendix B.1) to every proper isometry, screws and translations included. **[F]** With no overtwisted vertex both forms are exact, so Mir is seen only through overtwisted vertices, and with them all four combinations of class exchange and Mir occur among the exact operations. **[F]** On the defect-free CTM the singles are exact too: the complement X, the state reversal J_{state}, an involution that sends each routing table to its inverse and is exact as a reversal, and their product $X \circ J_{\mathrm{state}}$. **[F]**

Orbit of handedness and class. The handedness Υ and the class of the seed, the vertex where the lock's front starts, give four labels on one orbit (Fig. 6a). The product $t_{\mathrm{bc}} \circ \mathrm{Rot}_4$ exchanges the classes at fixed handedness, and $t_{\mathrm{bc}} \circ \sigma_d$ exchanges them, reverses the handedness and is exact with holds. The mirror σ_d alone reverses the handedness at fixed class and breaks at holds, since it flips the strand; Inv changes no label the rules read, so on the machine σ_d acts as Rot_2 and $t_{\mathrm{bc}} \circ \sigma_d$ as $t_{\mathrm{bc}} \circ \mathrm{Rot}_2$. The lock is therefore written alike from either seed class at either handedness. **[F]** The operations Mir and σ_d are distinct (Fig. 6a, b): σ_d reflects the positions and so the handedness, and Mir keeps both. **[F]**

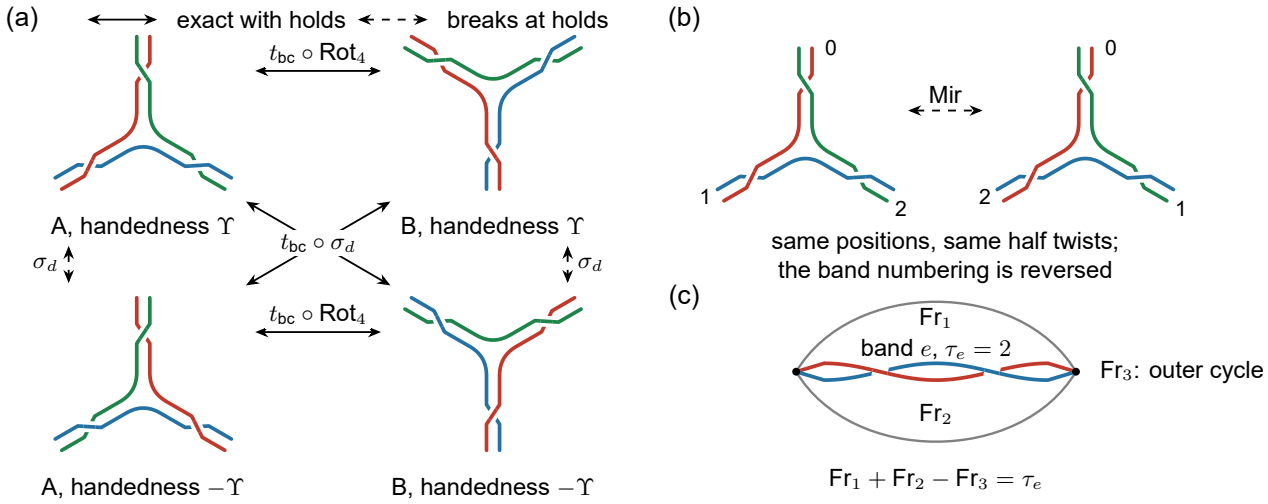


Figure 6: Handedness, class and framing. The icons are the bands of Fig. 2a, b without arrows or registers. (a) The four labels on one orbit; the lower row is the mirror image of the upper. (b) Mir reverses the band numbering at fixed positions and half twists. Solid arrows: exact with holds; dashed: breaks at holds. (c) One band e with two half twists in a theta graph; Fr_1 and Fr_2 are the framings of the two cycles that share only e, and Fr_3 that of the outer cycle.

Sign ledger. The label entries of Table 5, 12 operations by 7 labels, are recomputed from each operation's action on the machine labels; the last column, exactness with holds, comes from the checks above. **[F]** Both entries in distribution rest on that of J_{state} ($(-1.2 \pm 0.4) \times 10^{-4}$); the second follows because σ_d acts on the machine as Rot_2 and $t_{\mathrm{bc}} \circ \mathrm{Rot}_2$ is exact. **[Sim]** The overtwisted A and B vertices of a closure, a closed route through overtwisted vertices, differ in number by $3w$, with w its turning number. **[F]** The sign q is reversed by t_{bc} and kept by Rot_2 and J_{state}, hence kept by Rot_4,

which acts on every machine label as Rot_2 does, and by σ_d, since Inv changes no label the rules read; h is kept by every proper operation and reversed by Inv, σ_d and $t_{\mathrm{bc}} \circ \sigma_d$. **[F]** A walk sum along routes that weights each move out of an overtwisted vertex by $\exp(i\lambda\theta)$, with $\theta = \pm 2\pi/3$ the turn signed by the side of the band, reads at $\lambda = 1/2$ the sign -1 raised to the total framing around a loop, counted relative to the lock: an Aharonov–Bohm-type sign, one $\mathbb{Z}_2$ flux per loop (Section 5.1). **[F]**

Operation	class	χ	band order	Υ	h	w	bit value	with holds
t_{bc}	swap	$-$	$+$	$+$	$+$	$-$	$+$	breaks
Rot_4, Rot_2	$+$	$-$	$-$	$+$	$+$	$+$	$+$	breaks
Mir	$+$	$-$	$-$	$+$	$+$	$+$	$+$	breaks
X	$+$	$+$	$+$	$+$	$+$	$+$	$-$	breaks
J_{state}	$+$	$-$	$+$	$+$	$+$	$+$	$+$	in distribution
Inv	$+$	$+$	$+$	$-$	$-$	$+$	$+$	invisible
σ_d	$+^{\dagger}$	$-$	$-^{\dagger}$	$-$	$-$	$+$	$+$	breaks
$t_{\mathrm{bc}} \circ \mathrm{Rot}_4$	swap	$+$	$-$	$+$	$+$	$-$	$+$	exact
Mir $\circ\, \mathrm{Rot}_4$	$+$	$+$	$+$	$+$	$+$	$+$	$+$	exact
$t_{\mathrm{bc}} \circ \sigma_d$	swap†	$+$	$-^{\dagger}$	$-$	$-$	$-$	$+$	exact
$t_{\mathrm{bc}} \circ \sigma_d \circ J_{\mathrm{state}}$	swap†	$-$	$-^{\dagger}$	$-$	$-$	$-$	$+$	in distribution

Table 5: Sign ledger. Entries: $+$ kept, $-$ reversed, swap for A and B exchanged; a dagger marks an entry composed from the rows of the factors. Band order is the cyclic order of the bands at a vertex; Υ is the geometric handedness. Every operation is exact on the defect-free CTM, where J_{state} and the last row are reversals ($S \circ \mathcal{U} \circ S^{-1} = \mathcal{U}^{-1}$, S the operation, $\mathcal{U}$ the update) and the others commute with $\mathcal{U}$, carrying the pattern of overtwisted vertices along; the last column says whether it stays exact with holds on, "invisible" meaning that it changes no label the rules read: the Laves graph is chiral, so Inv maps the net to its mirror image. The route-charge sign q transforms as w on every row. **[F]**

C Machine specification

This appendix specifies the two machines as the code release runs them, each rule as one sentence with its file in a comment. L1 is the routing machine of Sections 3, 5 and 6, and L2 is the coarse machine of Sections 7 and 8. Rules are definitions and carry no grade; a property claimed of a rule does.

C.1 L1: the routing machine

State. A vertex has a class A or B and three darts, one on each of its bands, and a band $e = \{u, u'\}$ has two sides. Content is one bit, 0 or 1 with no label, in each of six registers per vertex, one on each side of each band end; readers and their windows are conventions of readout and are not part of the state (Section 5). The strand label of a register is $\chi = s \oplus [u \in \mathrm{B}]$, with s its side, u its vertex, $[u \in \mathrm{B}]$ the class bit and $\oplus$ exclusive or. Each dart carries one stop bit, so that $\tau_e = 1 + s_u + s_{u'}$ and $\delta_e = s_u \oplus s_{u'}$. A seat is a vertex whose three stops are all set, and only seats hold: a held pair is two bits off the registers, with an exit band, or none. The lock writes the stops of the initial pattern, and $f_u = 1$ marks a seat there. A seat also carries a step ledger, one label per dart, and an integer accumulator X_i, the state of the step decision below.

Routing and swap. A bit entering a vertex on arm b at side s leaves by arm $b + (2s - 1) \bmod 3$, whatever the stops. Crossing the band it changes side by $\tau_e \bmod 2$, that is $s \to s \oplus 1 \oplus \delta_e$ (the bit g_e of Appendix B.1), and a bit crossing by a swap changes side as if the band were untwisted, $s \to s \oplus \delta_e$; before the lock a bit keeps its side. The swap partner of a register is the register at the far end of its band, leaving by the mate dart on the other side, $s \oplus \delta_e$. A swap fires on a pair $\{a, b\}$ when both are occupied and the other pair $\{c, d\}$ of the band is both full or both empty; registers filled by an unhold

in this tick, and registers that a swapped bit would reach from them, take no part. Every free bit then moves on, by the swap crossing where a swap fires and by the normal crossing elsewhere.

Hold and unhold. Each tick, before anything else, every held pair is offered to its exit band: if both entry registers of that band are empty the pair is unheld into them and routed in this tick, and otherwise the exit band moves one slot on in the turning sense. This blocked advance is the only irreversibility of routing, swap and hold. **[F]** An empty seat then holds a pair arriving on both sides of one entry arm, not counting registers just filled by an unhold; both registers are emptied, and the arm is the exit band. If two arms qualify the seat holds on the one after the missing arm in the turning sense, and if three, none. A hold may be broken, its seat losing a stop, only after the pair has been unheld. A tick runs in order: holds, swaps, routing, the checks of the laws, and the move phase. The order within a tick, swap detection before routing, is a choice, and no rule of routing, swap or hold has a tunable parameter: the three bands, the two sides, one pair per seat and the turning sense are structural, and the pattern, the initial content and the schedule of the lock are inputs of a run. **[F]**

The glide. The move phase follows routing, and a seat moves by a two-bond step $v \to w \to v'$, one bond per tick, in which only stops move. The glide starts when the held pair of v, if any, has been unheld into its exit registers, which are then empty, when every stop in the shell around the step is clear, and when no other seat with a target within 1.6 cells starts at once. In tick 1 stops are set on the darts of w towards v and towards its third neighbour, and on the two darts of v' not towards w, so that δ is the coboundary of $\{v, w, v'\}$, only v is a seat, and N_{stop} goes from 3 to 7. In tick 2 the triple of v and the two stops of w are cleared and the dart of v' towards w is set, so that the triple stands at v' and N_{stop} is back at 3. A pair that v held in between is placed on the registers its held bits would reach by routing, the image unhold. If both images of a held bit are occupied, tick 2 waits, the glide keeping its intermediate state and trying again at the next move phase.

The step decision. Each seat keeps a step ledger, one label per dart, the side on which a stop label sits. After each tick, at each dart of the seat with exactly one of its two registers occupied, the bit and the label exchange sides if the occupied side differs from the label's; the bit count is unchanged. The seat's momentum is $M = \sum_x p(r_x) + p(r_1) + p(r_0)$, over the label registers r_x of its darts and the entry pair of the held band, and its energy is $E = 3 + 2[\text{held}]$, with $p(r)$ the unit route axis of r on the clean floor times $v_{\mathsf{bit}} = 1/4$. The velocity M/E accumulates in a position X, and the step d with the largest projection among the six second neighbours starts when $X \cdot d > |d|^2/2$, and then $X \to X - d$. In exact integers, $X_i = 60X$ is advanced by $X_i \to X_i + 15\, M_4/E$ with $M_4 = 4M$ a sum of signed axis vectors, the steps are $d = d_i/8$ with d_i even integers, $s_c = d_i \cdot X_i = 480\, X \cdot d$, the threshold reads $4\, s_c > 15|d_i|^2$, and the step $X \to X - d$ reads $X_i \to X_i - 15\, d_i/2$. The six candidates are $j = 2b + (c - 1)$, with b the first arm out of v and $c \in \{1, 2\}$ the turn at w. Among tied candidates the one is taken that precedes all the others in the rotation system's $+1$ sense, first by arm and then by turn; if none does, the three tied arms being cyclic, the seat waits one tick. This rule is stated as specification only.

C.2 L2: the coarse machine

Cells and stencils. Cells are the sites of the body-centred cubic lattice on a periodic box, class A at $2(i, j, k)$ and class B at $2(i, j, k) + 1$ in units of $a/2$, with volume 4 per site; each has eight hexagonal links to the other class, of weight $1/18$, and six square links to its own, of weight $1/36$, and twelve triangular faces, each of one square and two hexagonal links.

Fluid layer. Populations live on the rest state and the fourteen links, with weights $7/18$, $1/18$ and $1/36$ and $c_s^2 = 2/3$, with one relaxation time $\tau_{\mathsf{LB}} = 0.8$ for all stresses. The defect layer hops with attempt probability $p_a\, \alpha$ per tick, the lapse α gating it, in a direction chosen with the weights of the links, and p_a is set by the interface to L1 (below).

Tension layer. The scalar ψ obeys $\psi_{n+1} = 2\psi_n - \psi_{n-1} + V_2\, L\psi_n + s - g(\psi_n - \psi_{n-1})$, with $V_2 = 2$, the defect density s as source, $L\psi = \sum_i w_i(\psi(x+c_i) - \psi(x))$, and the damping $g = 0$ in the bulk and rising in a sponge near the faces of the box, where ψ is clamped to 0 on the outermost layer. For the static far-field test of a lump the source is its $T^{00} + \sum_i T^{ii}$ instead of the defect density (v6/l2/runs/clusters.py).

Frame layer. Each link carries a phase A_l with $\mu_l \ddot{A} = -C^T \kappa_f C A + J$, advanced by leapfrog with step 0.5: C takes the links of a face, $\mu_l = 1$ on hexagonal and $1/2$ on square links, and $\kappa_f = K_A = 1/2$, so that $c^2 = 4K_A/3 = 2/3$. Charges are smooth densities on the A sites, cubic B-splines along the motion, and the link currents are those of exact discrete continuity, $G^T J = \dot{Q}$, with temporal gauge, so that $CG = 0$ and the Gauss law holds at every step.

Lapse and ruler. With ψ given on the sites, its value on a link is the mean of the two ends and on a face the mean of its three links. The matched arm sets $\mu_l \to \mu_l e^{2\psi}$ and $\kappa_f \to \kappa_f e^{-2\psi}$; the clock arm $\mu_l e^{\psi}$ and $\kappa_f e^{-\psi}$; the mismatch arm $\kappa_f e^{-4\psi}$ with μ_l fixed. An emitter counts in its own ordinal $\nu_{\mathsf{s}} = \alpha_{\mathsf{s}} t$ at its seat.

Readers. A reader is a closure that counts and never writes the state: a seated aperture of sites, reading by the windowed transform in its own ordinal, and giving direction, deflection, delay and impact parameter from a lens run set against its flat twin. The event clock counts in its own ordinal and reads α; the cavity clock has a fixed chart size, a fixed link count, and reads α^2 (Section 8). The slit readouts use a fringe fit, and scattering uses tracked velocities against a point-particle reference.

Clusters. A complex carrier χ and a real binder σ on the sites have

$$\mathcal{L} = |\dot{\chi}|^2 - V_2 \sum_l w_l |\chi_h - e^{iqA_l}\chi_t|^2 - m^2|\chi|^2 - \xi|\chi|^6 + g\,\sigma|\chi|^2 + \tfrac{1}{2}\dot{\sigma}^2 - \tfrac{1}{2}V_2 \sum_l w_l(\Delta_l\sigma)^2 - \tfrac{1}{2}m_\sigma^2\sigma^2, \quad (14)$$

where the current $J_l = 2qV_2 w_l\, \mathrm{Im}(\bar{\chi}_h \Delta_l \chi)$ drives the frame layer. The standard cluster has $m = m_\sigma = 0.404$, $\xi = 0.149$, $g = 0.312$, the charge $q = 0.22$ per carrier and the carrier number $N = 380$, and a static lump is found at fixed N by imaginary-time relaxation. All layers share the speed c.

Interface and backgrounds. The link to L1 is structural: with the light speeds matched, $c\,a/T = c_0$ in L1 cells per L1 tick, L1 fixes only the product $a\,p_a = 3Dc/c_0$, with a the L2 cell in L1 cells, $D = (3.0571 \pm 0.0025) \times 10^{-3}$ from L1-b and c_0 the mean of 0.14432 ± 0.00012, 0.14434 ± 0.00008 and 0.14439 ± 0.00009 from L1-a. The runs take $p_a = 3Dc^2/(c_0^2 T)$ with $T = 1$ L1 tick per L2 tick, a declared choice; the other entries of Table 3 are comparisons only. A uniform background shifts ψ by a constant, and a stochastic background adds defects of strength 0.03 at random sites, a parameter, since L1 does not fix the global background offset it needs.

C.3 Engines and tests

L1 has three engines: a reference engine, one rule sentence per function, a vectorised engine and a bit-sliced GPU engine; the test file asserts that they agree bit for bit after every tick on random stops, holds and movers. Each tick the reference engine asserts single occupancy, the bit count, that routing is injective on occupied registers, the strand counts, the exact class charge q_{cl} after the move phase, and that every hold sits on a seat. Asynchronous schedules in which a band updates only when both its ends have done so agree with the synchronous run: before the lock, on 3- and 4-cell tori with random content, 12 of 12 schedules agree bit for bit, and with holds and swaps on 48 more agree, while 24 of 24 control schedules that do not wait for both ends fail. **[Sim]** L2 has one engine on NumPy or CuPy with the same code, and its test file asserts that the two agree within a stated tolerance.

D Methods and decisive tests

D.1 Methods

T1–T3. The three exhaustive runs use no randomness: T1 enumerates the routes, band families, windings and side covers on the finite Laves torus (3, 4 and 5 cells), T2 the symmetry operations on a 12-cell torus, the rule tables, the ledger entries and the frame group with its lift, and T3 the local maps behind the principles of Appendix A.1. A key is an exact count or identity and carries its expectation.

L1-a: the lock and the floor. L1-a runs the routing machine with one base seed, in sections: the lock front and the CTM on a 24-cell torus with 8 replicas, the dispersion of the count mode on 48 cells (192 replicas in 6 groups of 32, $k \le 0.95$), from which c_0 and the floor constants ν_0, ν_1 and ς are fitted, the phase line on 8 cells (2048 replicas, 3000 ticks), the asynchronous schedules on 3- and 4-cell tori, and the swap, charge and drag sections. A key is the mean over replica groups with its standard error.

L1-b: defects by the glide. L1-b runs glides on a 12-cell torus at occupancy $1/2$, with 4096 replicas in 16 groups and 10 000 ticks after a burn-in of 200; the class charge and the stop identity are checked on every tick for the first 64 and then every eighth. The hand-over coefficients are read from the seats' ledger velocity (Green–Kubo) and from the mean square displacement; the symmetry images are nine runs of 2048 replicas and 3000 ticks, the original and eight images, that share no content or ledger, and are compared by an F test.

L1-c: the ring of readers. L1-c reads a cluster of 20 seats on a 48-cell torus (64 cells for the moving run) with the windowed transform on shells of readers out to $r = 12$, for windows $\nu_{\mathsf{w}} = 4$, 6, 8 and 10 (the paper prints $\nu_{\mathsf{w}} = 8$; the window closes before the wrap-around while $\nu_{\mathsf{w}} < L/2 - r_{\mathsf{max}}$), in 64 batches whose errors come from 16 groups. The linear model takes the floor constants of L1-a. The excess of D10 is located by a re-reading of the stored chunks of the full run: it sits in the kept band next to the axial cut at the outer shells, the wake of the prescribed path (note (a) of the decisive tests), and the retarded reading stays excluded on the sectors $|\cos\theta| < 0.5$. The rms-z tolerance treated the shells as independent; with their measured correlation, from shared replicas, the central 99% chance band of the rms z reaches 2.10, and 2.38 stays outside it. **[Sim]** Clocks are read on closures at $r = 4$, 8, 10 and 12 on a 32-cell torus, 1500 ticks after a burn-in of 300 in 8 batches, with the cluster against without it, paired. The moving cluster is carried at about $0.44\,c_0$ for 275 ticks in both directions, and the dipole is read in 8 sectors of equal solid angle, as half the difference of the two runs, so that the shape bias of the cluster cancels.

L2-a: fields. L2-a runs the tension, frame and fluid layers on periodic boxes of 48 to 96 sites a side, with one seed: the Coulomb and Gauss tests with a point charge, the magnetic field of a moving charge, the field ψ of a static and a moving source, and the conservation and isotropy of the lattice-Boltzmann fluid. The Coulomb and ψ isotropy keys are read with the image field of the periodic box (Ewald for the frame layer, the clamped box for ψ) removed, and the box term is reported by itself as a measured key.

L2-b: light, clocks and sedimentation. L2-b sends a frame-layer pulse past a static ψ lump ($A_0 = 0.3$, impact parameters 8 to 24) for the deflection and the Shapiro delay, the lens tests using the rows of at least 4.2 Einstein radii, through a slab for the PPN parameter and the reflection, reads event and cavity clocks, and lets a density settle in a ψ well for 6×10^4 ticks between reflecting walls.

L2-c: slits, markers, eraser, floors. L2-c runs two slits 28 cells apart at wavelength 16 for both polarisations, with screens at 54, 80 and 108 cells and, in a larger box, at 160, 216 and 296 cells; markers of strength 0.05 and 0.12, the $\pm 45°$ eraser projections and a physical analyser layer; a uniform floor $\psi_{\mathsf{bg}} = 0.05$ and eight stochastic floors.

L2-d: clusters. L2-d relaxes a static cluster at five scales for the virial and the Tolman source, kicks it to $\gamma\beta = 0.5$, 1 and 2, scatters two clusters at impact parameters 40 and 20 and $\gamma\beta = 0.35$ and 0.75 with free-space controls, and applies a constant force.

Claim bases and tiers. Each key has a basis: theory, a prediction fixed before the run; internal, a conservation law, a control or a consistency check; measured, a value with its error and no expectation. A tolerance has one of five tiers: exact (integer or machine identity), stat (3 standard errors), disc (3 times the difference of a resolution pair, or of its Richardson extrapolation), design (a width fixed before the run) or deriv (from a stated relation). The disc tier applies only where a true resolution pair exists, L2-a, L2-b and L2-c, since a discretisation error is measured only by changing the resolution; the L2 runs come at three sizes, small, full and conv, each with twice the cells per side of the one before, and full and conv are the pair. The remaining 592 keys of the ten records are internal consistency checks or measured values that no claim rests on; all pass or carry no expectation, and all are listed in the release.

D.2 Decisive tests

Table 6 lists, by section, each claim that falls with its test, with its result and outcome; the three honest misses are printed as such. The readout keys of each row are listed in the record's README.

Row	§	Claim	Result	Outcome
D1	2	Every schedule that respects the causal order gives the same run	12/12; 48/48; the 24 control schedules fail	pass; control
D2	3	The lock mixes the content to $1/2$	99.2% mixed at lag 8; $\delta = (-5.3 \pm 0.3) \times 10^{-4}$; no front, 0% mixed	pass; control
D3	5	Register frames form O; the lift is the nonsplit $2O$	exhaustive	exact
D4	5	Floor stride $c_0 = v_{\mathrm{bit}}/\sqrt{3}$, three directions	0.14432 ± 0.00012, 0.14434 ± 0.00008, 0.14439 ± 0.00009 vs 0.14434; anisotropy $0.27\% \pm 0.06\%$ ($\leq 2\%$)	pass
D5	5	Floor constants handed to L2 and L1-c	$\nu_0 = 0.01084 \pm 0.00009$, $\nu_1 = 0.0387 \pm 0.0004$, $\varsigma = 0.0098 \pm 0.0012$	measured
D6	5	Holds write a phase-locked line, only holds do	27.7 s.e. (≥ 10); without holds 0.76 s.e. (≤ 3)	pass; control
D7	5.4	Ring of readers: Gauss's law	ratio 0.985 ± 0.006 (tol. 0.017); slope 0.003 ± 0.018 (tol. 0.054); rms z 0.80	pass
D8	5.4	No lapse on L1: clocks run at the far rate	rate shifts $\leq 1.2 \times 10^{-4}$, held-fraction shifts $\leq 2.2 \times 10^{-5}$ at $r = 4$–12, each within 3 s.e.	pass
D9	5.4	Moving source: the dipole is not at the retarded position	9.6 s.e. from the retarded position; controls 0.81 and 1.2 (tol. 1 ± 0.87)	pass; control
D10	5.4	Moving source: the outer-shell lag[a]	rms z 2.38 (tol. 1 ± 0.87)	**miss**
D11	6	Class charge exact; exact operations leave the statistics unchanged	0 violations; max $\lvert z \rvert$ 1.77 (Mir), 1.78 (t_{bc}), tol. 4.5; min p 0.71	pass
D12	6	No defect moves above c_0	fraction above 0 ($\leq 10^{-9}$); at c_0 0.0477	pass
D13	6	Defect diffusion D, handed to L2	$(3.0571 \pm 0.0025) \times 10^{-3}$ (Green–Kubo); $(3.1548 \pm 0.0025) \times 10^{-3}$ (displacement)	measured
D14	7	Exact Gauss law; Coulomb strength $1/(6\pi)$	residual 2.7×10^{-14} ($\leq 10^{-9}$); strength 1.0003 (tol. 6.6×10^{-4})	pass
D15	7	Coulomb potential isotropic, box images removed[b]	2.5×10^{-4} (tol. 6.4×10^{-4})	pass
D16	7	Biot–Savart law	1.04 ± 0.05 (tol. 0.14)	pass
D17	8.1	Light deflection over the ray-traced expectation[c]	1.024 full, 1.026 conv (tol. 0.021)	**miss**
D18	8.1	Shapiro delay over the finite-path eikonal[d]	0.978 full, 0.993 conv (tol. 0.045)	pass
D19	8.1	γ_{PPN} read on the slab	1.004 full, 1.002 conv (tol. 0.008); clock alone 0.010 (tol. 0.026)	pass; control

Table 6, continued

Row	§	Claim	Result	Outcome
D20	8.1	Event clocks read the lapse; sedimentation $n \propto e^{\psi}$	clock 2.4×10^{-5} (tol. 6.6×10^{-4}); slope 1.00000 (tol. 1.5×10^{-4})	pass
D21	8.3	Double slit, near field, polarisation Z along the slits	visibility 0.965–0.988; spacing 1.002, 1.001, 1.002 (tol. 6%)	pass
D22	8.3	Far-field fringe spacing, $L_s = 160, 216, 296$[e]	in $\lambda L_s/d$: 0.991, 0.988, 0.996; over the two-source slope 0.9905, 0.9886, 0.9947	**miss**
D23	8.3	A marker takes the visibility; a late marker equals none	0.839 vs 0.848 (tol. 0.0092); 0.492 vs 0.486 (tol. 0.027); late marker 1.9×10^{-4} (≤ 0.03)	pass
D24	8.3	The eraser restores the fringes, shifted by π; late choice	visibility 0.938 (≥ 0.9); phase 0.9996π (tol. 0.0048); late vs early 5.0×10^{-4} (≤ 0.05)	pass
D25	8.3	The stochastic floor decoheres without a which-path record	ensemble/mean visibility 0.551 (< 1); local coherence 0.954 (≥ 0.8)	pass
D26	8.4	Clusters: Lorentz relations, speed limit, Tolman source	$E/\gamma Mc^2$ 1.026 (tol. 0.030); $\beta_{\max}$ 0.657 (≤ 1); source/E 1.003 (tol. 0.010)	pass

Table 6: Decisive tests: the claim, its result against the expectation or tolerance, and the outcome.

Outcomes: pass, the value lies within its tolerance (tol.) or its threshold ($\leq$, $\geq$, $<$) in brackets; miss, it does not; exact, an exhaustive check; measured, a value reported with its error and no expectation; control, the row also prints a control, which is checked likewise. s.e. is standard error.

Notes.
(a) The lag fraction is 0.19 ± 0.06 against the damped linear model's 0.017: the lag exceeds the model. The excess sits in the kept cosine band next to the axial cut (0.5–0.75) at the outer shells $r = 7.5$–9.5, opposite in sign to the cut axial band: the wake of the prescribed path reaching past the cut at large r, which the linear model, holding only the store, does not contain. On the sectors $|\cos\theta| < 0.5$ the machine reads $\lambda = 0.07 \pm 0.12$ against the model's 0.07, and the retarded reading stays excluded. **[Sim]**
(b) The Coulomb deviation is taken with the continuum periodic-box image field removed; that box term alone is 5.6×10^{-4} (measured).
(c) Rows with $b \geq 4.2$ Einstein radii, where geometric optics holds; small has none. The 2.5% excess is the same at both resolutions and not explained.
(d) Along the traced ray, against the eikonal over the same finite path.
(e) Z, the field along the slits, passes at 216 and 296 but misses at 160 against the two-source slope (tol. 0.52%): 0.77% low after Richardson extrapolation, an offset that shrinks with L_s, not resolution. Y, the in-plane field across the slit width, is measured in the same units, 0.965, 0.961, 0.963, 3.5 to 3.9% low; the two-source prediction has no polarisation.

E Derivations

This appendix derives the results of Sections 5–9 that the text states without proof, one subsection for each part of the body that needs them; each paragraph says which claim it supports, opens with its premise, and grades its result.

E.1 Readings on L1

This subsection derives what Section 5 states without proof: the transform and its window law, the floor's stride, mass, charge and motion.

Step 3 of the windowed transform. For step (3) of the transform, Section 5. Premise: a weak signal in local equilibrium, the premise of Eq. (3): the far field of the source is locally a product state, each register holding 1 with probability $\frac{1}{2} + \varepsilon_s$, $|\varepsilon_s| \ll 1$. A degree-k Walsh character, the product of k register signs, then has expectation $(-2\varepsilon_s)^k$, so the degree-one term leads and higher terms are higher order in the signal. **[D]** For independent registers with one occupancy the count is a sufficient statistic for it (Fisher–Neyman), and the degree-one term is an affine function of the count, so reading it loses nothing about the mean signal; the expectation of the count is linear in ε_s, and the offsets

of independent weak sources add at leading order, which is superposition. **[D]** The wave term of bunching appears where the far field is not a product state, outside this premise.

Kac window law. For the window law of Section 5. Premise: a stationary, ergodic sequence of reader steps. Kac's lemma gives a configuration of probability μ per step a mean return time $1/\mu$. **[F]** For independent steps a window misses the event with probability $(1-\mu)^{\nu_{\mathsf{w}}}$, so missing it with probability at most ε needs $\nu_{\mathsf{w}} \geq \ln(1/\varepsilon)/\ln\bigl(1/(1-\mu)\bigr) \approx \nu_{\mathsf{Kac}} \ln(1/\varepsilon)$, plus the shortest hold, which is

$$\nu_{\mathsf{w}} \geq \nu_{\mathsf{w}}^{*} = \xi(j,\varepsilon)\, \nu_{\mathsf{Kac}} \ln(1/\varepsilon) + \nu_{\mathsf{d}}, \tag{15}$$

with $\nu_{\mathsf{Kac}} = 1/\mu$, ν_{d} the shortest hold and $\xi = \mu/\ln\bigl(1/(1-\mu)\bigr)$, 0.72 at $j=1$ and 0.99 at $j=6$ for $\mu = 2^{-j}$. **[F]** The departure of the machine's steps from independence is not measured here.

The floor's stride and the drift. For Eqs. (3) and (16). Premise: the floor is defect-free and in local equilibrium about a stationary measure. On the defect-free floor each tick is a bijection that conserves the number N and every strand difference along a route family, so a product measure in which each register's occupancy is a common parameter plus a drift parameter times the sign of its velocity is stationary; at $\rho = 1/2$ the common parameter vanishes at any drift, and the occupancy of the routes along $+a$ is ρ_a. **[F]** Given local equilibrium, number and lattice momentum obey $\partial_n N + \sum_a \partial_a \mathcal{P}_a = 0$ and $\partial_n \mathcal{P}_a + v_{\mathsf{bit}}^2\, \partial_a N_a = 0$; linearised about the measure, in which routes along $+a$ have occupancy ρ_a at $\rho = 1/2$, they give the stride along the unit wavevector $\hat{k}$,

$$c^2(\hat{k}) = v_{\mathsf{bit}}^2\, \frac{\sum_a \hat{k}_a^2\, \rho_a(1-\rho_a)}{\sum_b \rho_b(1-\rho_b)}, \tag{16}$$

and at rest, with $N_a = N/3$, Eq. (3). **[D]** For a drift βc_0 along a cube axis, Eq. (16) gives the strides along and across it, $c_{\parallel}^2 = c_0^2(1-3\beta^2)/(1-\beta^2)$ and $c_{\perp}^2 = c_0^2/(1-\beta^2)$. **[D]** A drift is a motion of the flow over the graph, not of the floor, and serves only to test Eq. (16) at Euler order [40].

Held store and Gauss's strength. For Eqs. (4) and (5). Premise: the count density u of the floor responds linearly, by the damped wave equation $\partial_t^2 u + \Gamma\, \partial_t u - c_0^2 \nabla^2 u = s(\mathbf{x}, t)$. A held pair leaves the registers for its dwell, so over a run the number held is, by Little's law [41], the rate of holds times the mean dwell, a count of seats and of held pairs that adds over sources whatever the shape of the closure. **[D]** A held pair is a hold and an unhold in time, a source $s = \delta^3(\mathbf{x})\,[\delta(t-\tau) - \delta(t)]$ for a dwell τ; a constant source would not do, since N is conserved and the zeroth time moment of u vanishes. The first time moment $S_1(\mathbf{x}) = \int t\, u\, dt$ then obeys $-c_0^2 \nabla^2 S_1 = H\, \delta^3(\mathbf{x})$, Eq. (4), with H the rate times the dwell: the ∂_t^2 term integrates to zero, and the Γ term gives $-\Gamma$ times the zeroth moment, which is zero. So $S_1 = H/(4\pi c_0^2 r)$, and the windowed deficit of a reader at distance r, once the window has outrun the damping's range, gives $r S_1 \to H/(4\pi c_0^2)$, Eq. (5). **[D]**

The charge sign. For Eq. (6). Premise: first order in λ. The turn at a vertex multiplies the flow by $e^{i\lambda\sigma_v 2\pi/3} = 1 + i\lambda\sigma_v 2\pi/3 + O(\lambda^2)$, so at first order the response of a source with route-charge sign q_{s} is $i q_{\mathsf{s}} e_1$ and that of a reader $i q_{\mathsf{r}} e_1$, with one real $e_1 > 0$. The composed reading multiplies the two imaginary factors, $-q_{\mathsf{s}} q_{\mathsf{r}} e_1^2$, whose sign is Eq. (6). **[D]** Taking the composed reading as minus the interaction energy is a choice, with the physics that like charges repel; the compared reading puts the reader's own response against the arriving one, so enters it conjugated, which reverses an imaginary factor, and has the opposite sign. **[Rev]**

Rate law. For (i)–(iii) of Proposition 1. Premise: readers and sources are interchangeable (Appendix A.1), so a party moves relative to the floor, with signals at an isotropic c_0, and its ordinal advances at a fraction f of its rest rate. A seated reader and a source receding at β exchange the factor $1-\beta$ over f out and f over $1+\beta$ back, and radar reciprocity sets them equal, so $f = \sqrt{1-\beta^2} = 1/\gamma$, which is (i). **[D]** Proper counts then give the Doppler factor $\mathcal{D}$ of (ii), and the lossless wave equation is Lorentz covariant, so a uniformly moving source has the Heaviside field of (iii), a function of the distance in the source's rest frame. **[D]**

E.2 Fields and clocks on L2

This subsection derives what Sections 7 and 8 state without proof: the fields on the cells, the lapse and ruler, delay and clocks, and the Tolman source.

Fields on the cells. For Eq. (8) and the Coulomb potential of the frame layer, Section 7. Premise: at long range the discrete operators are their continuum limits. The Laplacian of the tension layer is $L = \nabla^2/3$ to leading order, since $\sum_i w_i c_{ix}^2 = 2/3$; a source s at one site has the density $4s\,\delta^3$, and $(V_2/3)\nabla^2\psi = -4s\,\delta^3$ gives Eq. (8), $\psi = 3s/(\pi V_2 r)$. **[D]** The frame operator is $G^T\mu G = -6\nabla^2$ in the same units, so the potential of a charge q obeys $-6\nabla^2\phi = 4q\,\delta^3$ and is $q/(6\pi r)$. **[D]**

Lapse, ruler and delay. For Eqs. (10) and (11) and the clocks of Section 8. Premise: the declared lapse and ruler, $\alpha\varrho = 1$. Waves on the frame layer have $c^2 \propto \kappa_f/\mu_l$ and impedance $Z \propto \sqrt{\kappa_f\mu_l}$. The matched arm, $\mu_l e^{2\psi}$ and $\kappa_f e^{-2\psi}$, leaves Z unchanged, so a ray is not reflected, and has the local speed $c\,e^{-2\psi}$, which gives the delay of Eq. (10) with $\gamma_{\text{PPN}} = 1$; the clock arm, $\mu_l e^{\psi}$ and $\kappa_f e^{-\psi}$, leaves Z unchanged with the speed $c\,e^{-\psi}$, which is $\gamma_{\text{PPN}} = 0$; the mismatch arm, $\kappa_f e^{-4\psi}$ alone, has the speed of the matched arm and changes Z, and so reflects. **[D]** For $\psi = A_0/r$ the index $n = e^{(1+\gamma_{\text{PPN}})\psi}$ bends a ray at impact parameter b by $\int \partial_b n\, dz = 2(1+\gamma_{\text{PPN}})A_0/b$ and delays it by $(1+\gamma_{\text{PPN}})\int \psi\, dz/c$, whose slope in $\ln b$ is $-2(1+\gamma_{\text{PPN}})A_0/c$, Eq. (11). **[D]** The matched arm puts the speed into both weights, $\mu_l \to \mu_l e^{2\psi}$ and $\kappa_f \to \kappa_f e^{-2\psi}$, discrete Hodge stars of length to the power ± 1. An event clock counts in its own ordinal αt, so a signal of the source's frequency is read at the ratio $\alpha_{\text{s}}/\alpha_{\text{r}}$; a cavity of fixed chart size, a fixed link count ℓ, has the frequency $c_{\text{local}}/\ell \propto e^{-2\psi}$, the lapse squared, and one of fixed proper length has the chart size $\ell \propto e^{-\psi}$ and so the frequency $\propto e^{-\psi}$, the lapse. **[D]**

Von Laue and Tolman. For the Tolman source of the static far-field test, Section 7. Premise: a static closed body, so $\partial_j T^{ij} = 0$, and $\partial_j(T^{ij}x^k) = T^{ik}$ integrates to $\int T^{ik}\, d^3x = 0$, so $\int (T^{00} + \sum_i T^{ii})\, d^3x = \int T^{00}\, d^3x = E$: the source of the rigid layer's far field is the total energy, whether the lump is charged or neutral. **[D]**

E.3 Reassembly: Maxwell and the weak-field static Einstein equations

This subsection assembles the parts of Section 7: Maxwell's equations in full, and Einstein's only in the weak-field static sector.

Maxwell. For the frame layer, Section 7. Premise: the continuum limit at long range, and the isotropy of rank 2 of the link weights, $\sum_l \mu_l\, v_i v_j \propto \delta_{ij}$, which the cubic stencil forces. **[F]** Take $\mathbf{E} = -\partial_t A$ on links, the temporal gauge, and $\mathbf{B} = CA$ on faces. Three identities are exact on the cells. The identity $CG = 0$ gives, with $G^T J = \dot{Q}$, the Gauss law $G^T\mu A' = Q - \bar{Q}$ at every step. Every link of a closed surface of faces bounds two faces of opposite orientation, so $\nabla\cdot\mathbf{B} = 0$; and $\partial_t B = -C\mathbf{E}$ is Faraday's law. The leapfrog update $\mu_l\ddot{A} = -C^T\kappa_f CA + J$ is Ampère's law, with $\varepsilon_0 = 3/2$ from the link inertia per cell of volume 4, the strength of $q/(4\pi\varepsilon_0 r) = q/(6\pi r)$ in Appendix E.2, and $1/\mu_0 = 2K_A$ from the face stiffness, so that $c^2 = 1/(\varepsilon_0\mu_0) = 4K_A/3$, **[D]** and the four equations are

$$\begin{aligned} \nabla\cdot\mathbf{E} &= \frac{\rho}{\varepsilon_0}, \qquad & \nabla\cdot\mathbf{B} &= 0, \\ \nabla\times\mathbf{E} &= -\partial_t\mathbf{B}, & \nabla\times\mathbf{B} &= \mu_0\mathbf{J} + \frac{1}{c^2}\,\partial_t\mathbf{E}. \end{aligned} \tag{17}$$

The value $K_A = 1/2$ is the declared choice of one speed for every layer. **[Rev]** Rows D14 to D16 of Table 6 check the Gauss residual, the Coulomb strength and the Biot–Savart ratio.

The weak-field static Einstein equations. For the lapse, the ruler and the Tolman source of Section 7, and the metric of Section 8.1. Premise: the declared lapse and ruler of Eq. (9) and the Tolman source of the static cluster test. **[Rev]** The clocks and rulers of the readers give the static line element

$ds^2 = -\alpha^2 c^2 dt^2 + \varrho^2 |d\mathbf{x}|^2$, which to first order in ψ is $g_{00} = -(1-2\psi)$, $g_{ij} = (1+2\psi)\delta_{ij}$. With $\Phi = -\psi$ this is the static, isotropic solution of the linearised field equations outside the source, $g_{00} = -(1+2\Phi)$, $g_{ij} = (1-2\Phi)\delta_{ij}$, with $\gamma_{\mathsf{PPN}} = 1$ and the 00 equation $\nabla^2\Phi = (4\pi G_{\mathsf{N}}/c^4)(T^{00} + \sum_i T^{ii})$ in the Tolman form. The static tension layer obeys $\nabla^2\psi = -(12/V_2)\, s$, the form of Eq. (8) for a source density s, the defect density in the runs and $T^{00} + \sum_i T^{ii}$ in the static cluster test, so $\nabla^2\Phi = (12/V_2)\, s$ is the same equation. **[D]** The strength $12/V_2$ stands for $4\pi G_{\mathsf{N}}/c^4$; the machine fixes no G_{N}. **[L]** Deflection, delay and redshift follow (Section 8.1, rows D17 to D20 of Table 6). **[D]**

What is not reached. Not reached are tensor modes, gravitational waves and frame dragging, since the tension layer is one scalar, so L2 is a scalar metric theory that agrees with general relativity in the weak-field static sector and not beyond it; **[D]** the nonlinear field equations of general relativity, and $\beta_{\mathsf{PPN}} = 1$, which the exponential form declares and no run tests; and clusters as dynamical sources and in free fall (Section 9.2).

E.4 Counting and cosmology

This subsection derives what Section 9.1 states without proof: the two statistics of a counting reader and the readout cosmology.

Bunching in a resolution cell. For the two statistics of Section 9.1. Premise: a cell holds M independent modes of mean intensity $\bar{I}$, each counted as Poisson at its intensity. For the collective mode, a nearly Gaussian sum, each I_i is exponential, $\langle I_i^2 \rangle = 2\bar{I}^2$, so $\langle n_{\mathsf{c}}(n_{\mathsf{c}}-1)\rangle = M(M+1)\bar{I}^2$ and $g^{(2)}(0) = 1 + 1/M$; for M single registers, each holding 1 with probability ρ, only distinct sites pair and $g^{(2)}(0) = 1 - 1/M$. **[F]**

Readout cosmology. For Eq. (13) and the claims of Section 9.1. Premise: light runs at c_0 in cells per network tick at every n, and with its speed fixed in reader units one conformal factor serves every unit. So n is read as conformal time η, a reader cell is b network cells on a side, reader time is $dt = d\eta/b$, the scale factor is $a = 1/b$ and $H = -db/d\eta$. **[Rev]** The conformal Friedmann equation of general relativity for $k = 0$, $(a')^2 = \mathcal{C}_{\mathsf{m}}\, a + \mathcal{C}_\Lambda\, a^4$ with $' = d/d\eta$, becomes with $a = 1/b$ the form of Eq. (13). **[Rev]** Its derivative $b'' = \frac{3}{2}\,\mathcal{C}_{\mathsf{m}}\, b^2$ holds no $\mathcal{C}_\Lambda$, a first integral, and $(1/b)'' = \frac{1}{2}\mathcal{C}_{\mathsf{m}} + 2\,\mathcal{C}_\Lambda\, b^{-3} > 0$. **[D]** Since $H > 0$ and $(1/b)'' > 0$, the scale factor $1/b$ is increasing and convex in η and never saturates, whatever the share of the constant. **[D]** When $\mathcal{C}_{\mathsf{m}} b^3 \ll \mathcal{C}_\Lambda$, $-db/d\eta \to \sqrt{\mathcal{C}_\Lambda} \equiv H_\Lambda$, so that $b = H_\Lambda(\eta_\infty - \eta)$, $H_\Lambda^{-1} = (\eta_\infty - \eta)/b$, and with $dt = d\eta/b$, $b \propto e^{-H_\Lambda t}$ and $H^2 - H_\Lambda^2 = \mathcal{C}_{\mathsf{m}} b^3 \propto e^{-3H_\Lambda t}$ to leading order, with the fixed point $H = H_\Lambda$ of de Sitter; the knee $\mathcal{C}_{\mathsf{m}} b^3 = \mathcal{C}_\Lambda$ is $H^2 = 2H_\Lambda^2$. **[Rev]** If a reader tick is at least one network tick, b cannot fall below 1, and the continuum equation fails where b stops, since $\mathcal{C}_\Lambda > 0$ forbids $b' = 0$. **[Rev]** If Newton's constant is a number times the area of a network cell, which is b^{-2} in reader units, then $d \ln G_{\mathsf{N}}/dt = 2H$. **[D]**

E.5 Bell correlations at the readout layer

This subsection supports the sentence of Section 9.1 that a path leads from the $\lambda = \frac{1}{2}$ channel to Bell correlations, at the readout layer and for seated readers; no machine runs it, since L1 has no walk-sum engine and no event that writes a pair.

The walk sum. Premise: a flow's $\lambda = \frac{1}{2}$ component propagates by the mean dynamics, a product-measure walk, under the local equilibrium of Eq. (3). **[D]** Walk weights, products of step probabilities of the routing-and-swap matrix and a survival factor per step, are positive. **[F]** The base frame transport is flat, since frames are register attributes, so a walk carries $\hat{U}(\gamma) = s(\gamma)\,\hat{U}_0$ with $\hat{U}_0$ fixed by its ends and $s = \pm 1$ the sheet sign, a homomorphism from closed walks to $\mathbb{Z}_2$. The $\lambda = \frac{1}{2}$ kernel is therefore $K = Z\,\rho(\hat{U}_0)$, with ρ the spin representation of $2O$ and $Z = W_+ - W_-$ the difference of the weights of walks arriving on the two sheets: the measure is positive on the cover and signed only on projecting

to the base. **[F]** The ratio Z/W, with $W = W_+ + W_-$, is the coherence of one flow: the ten-rings lift open (Appendix B.1), so the $\mathbb{Z}_2$ system is not a gauge even on the defect-free floor, and by Wielandt's theorem [42] $|Z| < W$ for long walks, so Z/W falls with distance. **[D]**

The pair. The seated source's base frame is fixed and the base transport is flat, so the two flows leaving it differ only by a sheet sign. **[F]** Over many events their relative sheet has mean $V > 0$, the pair coherence: the parity coherence of the source's circulations times a function of the two flows' Z/W, a machine number not yet measured; the single-event version is $V = 1$. **[Conj]** Each event's pair tensor has weight 0, chosen to match a pair from a source of zero angular momentum, and the count is the weight-0 pairing of the amplitude with its conjugate. **[Rev]** The pair tensor is then the projector on the invariants of the tensor square of the spin representation, which are one-dimensional and antisymmetric because the extension is nonsplit, so ρ is quaternionic: the singlet, unique. **[F]** Here "many events" means that each flow is many causal units carrying one modulation, the walk sum itself, so these per-event claims hold.

The correlation. A reader's setting is an oriented axis of its frame that carries a half turn, an element u of order 4 in $2O$; there are 18, six along the fourfold axes and twelve along the arrival directions, and the outcome ± 1 is $i\rho(u)$. **[F]** Readers a and b read

$$E = -\tfrac{V}{2}\,\chi_{1/2}\big(u_a u_{b'}^{-1}\big) = -V\cos\theta, \tag{18}$$

with $\chi_{1/2}$ the $\lambda = \frac{1}{2}$ character, $u_{b'}$ the axis u_b carried into the frame of a and θ the angle between the axes compared along the flow, and each marginal is $\frac{1}{2}$ at every V, so there is no signalling. On the network's frames $\theta \in \{0, 45, 60, 90, 120, 135, 180\}^\circ$, and the CHSH sum S reaches $\frac{5}{2}V$ with settings on the arrival directions and $2\sqrt{2}\,V$ when the fourfold axes are used too. **[F]** Tsirelson's bound [43] is the limit for any reading of this form. **[D]**

Resolved and aggregate readings. Premise: the reader's window resolves one pair event. **[Conj]** Then, for the Tsirelson settings, no positive joint distribution over the four outcomes reproduces the four pair tables exactly when $V > 1/\sqrt{2}$ [44], so the bound 2 of CHSH [45] and Bell [46] does not bind the readout layer. **[D]** A reading that aggregates many pair events per window keeps the cosine shape of count fluctuations, $-V\cos\theta$, but its CHSH value is at most $2\sqrt{2}\,V/k$ for k events and in the many-event limit a positive Gaussian joint exists, so it carries no signed-measure claim. **[D]** The chain takes its weakest link, the pair coherence $V > 0$ and, for the signed-measure claim, event resolution at the reader. **[Conj]**

F Notation

Table 7 lists the symbols that recur, that this paper introduces, or that it uses in a sense of its own; standard symbols in their usual sense are defined where they appear.

Symbol	Meaning	§
L1: structure and machine		
T^3; A, B	the three-torus; the two vertex classes	2
n	network tick, a local causal ordinal	2
ρ	occupancy, the fraction of registers holding 1	2
s; s_u	side of a band; stop bit of a dart	3, C
e; u, u'	a band; its two ends	3
χ; χ_0, χ_1	strand label $s \oplus [u \in \mathrm{B}]$; the two strands	2, C.1
Υ	handedness of the lock's half twists, ± 1	3
τ_e; δ_e	number of half twists on band e; parity of the extra twist	3, C
f_u; rot_u; g_e	seat bit; rotation-system bit; routing bit	B, C
p	density of overtwisted vertices	5
δ	offset of each side's composition from $1/2$ after the lock's mixing	3

Table 7, continued

Symbol	Meaning	§
E	number of bands	6
N_{stop}; n_{def}; q_{cl}	number of stops; number of defects; class charge $n_{\text{A}} - n_{\text{B}}$	6
w	closure index, the turning number of a closed route	5, B
h; q	band-rotation sign, named helicity; route-charge sign, named charge sign	4
λ	phase weight, named spin weight	5
a	cube-axis index	E
N; Q	number density; strand-difference density	A.1
v_{bit}; c_0	bit stride; stride of the floor's collective mode, $v_{\text{bit}}/\sqrt{3}$	5
Γ; ν_0, ν_1, ς	damping of the floor's mode; the isotropic and cubic parts of its damping and the dispersion coefficient	5, E
D; τ_v; μ_n	defect diffusion; velocity memory; content-gradient mobility	6
$p(r)$	momentum of one register, the unit route axis times v_{bit}	C
X, X_i	position of a seat in cells; its integer form $60X$	C
Operations and names		
t_{bc}	body-centre translation, exchanging A and B	4
Rot_4; Rot_2	fourfold screw rotation; twofold rotation	4
Mir; Inv; σ_d	reversed rotation system; inversion; diagonal mirror Inv $\circ$ Rot_2	4
$\mathcal{U}$	the update	B.3
X	complement, $0 \leftrightarrow 1$ in every register	4
J_{hist}; J_{state}	causal reversal; state reversal	4
C, P, T	names of t_{bc}, σ_d, J_{state}	4
Readout		
S^2; $\hat{n}$	the sky of a reader, the sphere of directions of the flow lines through it; a direction on it	5
ν; ν_{d}; ν_{w}; ν_{s}	the reader's own ordinal; shortest hold; window length; an emitter's ordinal	5, C
ω; ω_0; $\overline{h}$	demodulation frequency; frequency at the source's own ordinal; reduced Planck constant	5, 8
$X(\omega, \nu)$	windowed transform of a reader's counts	5
τ	dwell of a held pair	5
H; u; S_1	held store; count density of the floor; first-moment reading	5
β; φ; γ; $\mathcal{D}$	speed in units of c_0, $\beta = \lvert\tanh\varphi\rvert$; rapidity; $(1-\beta^2)^{-1/2}$; Doppler factor	5
ε_{s}	offset of a weak source's occupancy from $1/2$	5, E
θ; σ_v	turn at a vertex, $\pm 2\pi/3$; class sign of a vertex	5
V; θ	pair coherence; Bell angle	9, E.5
E	correlation of two readers' outcomes	E.5
$\bar{n}$; M	mean count in a resolution cell; modes in it	9
N_{eff}	effective number of samples of a window	5
j; μ; ν_{Kac}	registers read jointly; probability per reader step; mean return time $1/\mu$	5, E
ε; ξ	tolerance of a window; prefactor of the window law	5, E
L2		
ψ; s	tension, gravity's field; strength of its source	7
α; ϱ	lapse $e^{-\psi}$; ruler e^{ψ}, with $\alpha\varrho = 1$	7
γ_{PPN}, β_{PPN}; A_0	PPN parameters, 1 in the matched medium; far-field amplitude of a mass	7, 8
V_2; K_A	stiffness of the tension layer; face stiffness of the frame layer	7, C
c; c_s	speed of every layer; speed of sound of the fluid	7, C.2
a; p_a; T	L2 cell in L1 cells; hop probability of the defects on L2; L1 ticks per L2 tick, a declared choice	7, C
A_l; B	phase on a link; flux through a face	C.2
μ_l; κ_f	link weight; face weight, matched to the impedance	7, C
G; C	discrete gradient; discrete curl	7, C
τ_{LB}	relaxation time of the lattice Boltzmann fluid	C
χ; σ; q; N	carrier and binder of a cluster; charge per carrier; carrier number	7, C
$\mathbf{E}$; ε_0; μ_0	electric field; permittivity and permeability of the frame layer in cell units	E.3
Φ; G_{N}	weak-field potential $-\psi$; Newton's constant	E.3, 9
E; M	energy of a lump; its rest mass E_0/c^2	7, 8
b; L_{s}; θ	impact parameter; distance to the screen; scattering angle	8
κ	deflection of a ray, $2(1+\gamma_{\text{PPN}})A_0/b$	8.1
τ	strength of a marker, τ_2	8.3
Cosmology		
b; η	reader tick length in network ticks; conformal time	9, E

Table 7, continued

Symbol	Meaning	§
$\mathcal{C}_\Lambda$, $\mathcal{C}_\mathsf{m}$; Λ	constants of the readout Friedmann equation; the cosmological constant, a first integral	9
H; H_Λ	Hubble rate $-db/d\eta$; its late-time value $\sqrt{\mathcal{C}_\Lambda}$	9, E

Table 7: Symbols and the section or appendix that defines them.

Data and code availability

The code release runs the machine of Appendix C and the runs of Appendix D; it needs Python 3.11 or later, NumPy and SciPy. The code and the run records are in one deposit, doi:10.5281/zenodo.24013013. It holds the v6 machine code (L1, L2, the topology proofs T1–T3, the run tables and the tests), one readout file in JSON for each run with its values, errors, tolerances and guard summaries, the sufficient-statistics records, and SHA-256 hashes of the archives and of every run record. A README in the record gives the layout, the run for each readout and how to run it. Every key cited in the text is in those readouts.

Acknowledgments

The author thanks the community of theoretical physicists and mathematicians on whose concepts this construction is built. The picture the author keeps returning to is the elephant in a dark room: the programs that look beneath spacetime each hold something that is really there, and the difficulty is the dark. This paper borrows their abstractions, those Section 10 names, and reassembles them by physical intuition into one construction, trying to set each piece at the level where it belongs and to find what is still missing between them.

The author thanks Anthropic and Google for the AI tools used here: the Claude Fable, Opus and Sonnet families, used in turn as tasks required, and Gemini 4 Argon, for theoretical exploration.

Author contributions

The human author holds the picture and its intuition, the ontological choices and the outermost decisions, taken at checkpoints: scope, title, tone and the frame of the readings. A nested team of Claude agents unfolds that picture and its tasks layer by layer: an integrating session holds the middle layer, the rulings and the specification, and agents with their own context hold details and implementation. In research the team alternated breadth, widening the map, with depth, carrying candidates to a checkable end; it implemented and ran the machine, derived results, audited claims against the machine's readouts and retrieved mathematics and physics, and it proposed candidates, which the author accepted, revised or rejected. In writing, a Writer held the text, an Editor checked it, cold-read sessions, without the project's context, read the drafts, and the integrating session ruled. Claude models also corrected English grammar and wording, improved fluency, drew the figures and edited the LaTeX source. The human author reviewed all AI-generated content and takes full responsibility for the published article.

References

[1] K. Zuse, *Rechnender Raum*, Schriften zur Datenverarbeitung, Vol. 1 (Vieweg, Braunschweig, 1969).

[2] E. Fredkin, Digital mechanics: an informational process based on reversible universal cellular automata, *Physica D* **45**, 254–270 (1990).

[3] C. Barceló, S. Liberati and M. Visser, Analogue gravity, *Living Rev. Relativ.* **14**, 3 (2011).

[4] H. S. M. Coxeter, On Laves' graph of girth ten, *Canad. J. Math.* **7**, 18–23 (1955).

[5] M. O'Keeffe, M. A. Peskov, S. J. Ramsden and O. M. Yaghi, The Reticular Chemistry Structure Resource (RCSR) database of, and symbols for, crystal nets, *Acc. Chem. Res.* **41**, 1782–1789 (2008).

[6] A. F. Wells, *Three-Dimensional Nets and Polyhedra* (Wiley, New York, 1977).

[7] T. Sunada, Crystals that nature might miss creating, *Notices Amer. Math. Soc.* **55**, 208–215 (2008).

[8] H. Bondi, *Relativity and Common Sense* (Anchor Books, Doubleday, Garden City, N.Y., 1964).

[9] A. Einstein, Zur Elektrodynamik bewegter Körper, *Ann. Phys.* **17**, 891–921 (1905).

[10] S. Chadha and H. B. Nielsen, Lorentz invariance as a low energy phenomenon, *Nucl. Phys. B* **217**, 125–144 (1983).

[11] L. Bombelli, J. Henson and R. D. Sorkin, Discreteness without symmetry breaking: a theorem, *Mod. Phys. Lett. A* **24**, 2579–2587 (2009).

[12] M. Kac, On the notion of recurrence in discrete stochastic processes, *Bull. Amer. Math. Soc.* **53**, 1002–1010 (1947).

[13] J. Hardy, Y. Pomeau and O. de Pazzis, Time evolution of a two-dimensional model system. I. Invariant states and time correlation functions, *J. Math. Phys.* **14**, 1746–1759 (1973).

[14] U. Frisch, B. Hasslacher and Y. Pomeau, Lattice-gas automata for the Navier–Stokes equation, *Phys. Rev. Lett.* **56**, 1505–1508 (1986).

[15] G. Nordström, Zur Theorie der Gravitation vom Standpunkt des Relativitätsprinzips, *Ann. Phys.* **42**, 533–554 (1913).

[16] G. M. D'Ariano and P. Perinotti, Derivation of the Dirac equation from principles of information processing, *Phys. Rev. A* **90**, 062106 (2014).

[17] M. Henneaux and C. Teitelboim, The cosmological constant and general covariance, *Phys. Lett. B* **222**, 195–199 (1989).

[18] W. G. Unruh, Unimodular theory of canonical quantum gravity, *Phys. Rev. D* **40**, 1048–1052 (1989).

[19] S. Weinberg, The cosmological constant problem, *Rev. Mod. Phys.* **61**, 1–23 (1989).

[20] Planck Collaboration, Planck 2018 results. VI. Cosmological parameters, *Astron. Astrophys.* **641**, A6 (2020).

[21] T. Jacobson, Thermodynamics of spacetime: the Einstein equation of state, *Phys. Rev. Lett.* **75**, 1260–1263 (1995).

[22] M. J. W. Hall, Local deterministic model of singlet state correlations based on relaxing measurement independence, *Phys. Rev. Lett.* **105**, 250404 (2010).

[23] G. Spencer-Brown, *Laws of Form* (Allen and Unwin, London, 1969).

[24] T. Toffoli and N. Margolus, *Cellular Automata Machines: A New Environment for Modeling* (MIT Press, Cambridge, MA, 1987).

[25] G. 't Hooft, *The Cellular Automaton Interpretation of Quantum Mechanics* (Springer, Cham, 2016).

[26] R. Landauer, Irreversibility and heat generation in the computing process, *IBM J. Res. Dev.* **5**, 183–191 (1961).

[27] M. Z. Guo, G. C. Papanicolaou and S. R. S. Varadhan, Nonlinear diffusion limit for a system with nearest neighbor interactions, *Commun. Math. Phys.* **118**, 31–59 (1988).

[28] G. Gallavotti, Divergences and the approach to equilibrium in the Lorentz and the wind-tree models, *Phys. Rev.* **185**, 308–322 (1969).

[29] C. Boldrighini, L. A. Bunimovich and Ya. G. Sinai, On the Boltzmann equation for the Lorentz gas, *J. Stat. Phys.* **32**, 477–501 (1983).

[30] R. Penrose, Twistor algebra, *J. Math. Phys.* **8**, 345–366 (1967).

[31] J. A. Wheeler, Information, physics, quantum: the search for links, in *Complexity, Entropy, and the Physics of Information*, edited by W. H. Zurek (Addison-Wesley, Redwood City, CA, 1990), pp. 3–28.

[32] C. W. Misner, K. S. Thorne and J. A. Wheeler, *Gravitation* (Freeman, San Francisco, 1973), Chap. 44.

[33] R. Penrose, Angular momentum: an approach to combinatorial space-time, in *Quantum Theory and Beyond*, edited by T. Bastin (Cambridge University Press, Cambridge, 1971), pp. 151–180.

[34] L. Bombelli, J. Lee, D. Meyer and R. D. Sorkin, Space-time as a causal set, *Phys. Rev. Lett.* **59**, 521–524 (1987).

[35] S. Wolfram, A class of models with the potential to represent fundamental physics, *Complex Syst.* **29**, 107–536 (2020).

[36] T. Konopka, F. Markopoulou and S. Severini, Quantum graphity: a model of emergent locality, *Phys. Rev. D* **77**, 104029 (2008).

[37] J. Ambjørn, J. Jurkiewicz and R. Loll, Emergence of a 4D world from causal quantum gravity, *Phys. Rev. Lett.* **93**, 131301 (2004).

[38] A. Bisio, G. M. D'Ariano, P. Perinotti and A. Tosini, Free quantum field theory from quantum cellular automata: derivation of Weyl, Dirac and Maxwell quantum cellular automata, *Found. Phys.* **45**, 1137–1152 (2015).

[39] J. A. Ellis-Monaghan and I. Moffatt, *Graphs on Surfaces: Dualities, Polynomials, and Knots* (Springer, New York, 2013).

[40] U. Frisch, D. d'Humières, B. Hasslacher, P. Lallemand, Y. Pomeau and J.-P. Rivet, Lattice gas hydrodynamics in two and three dimensions, *Complex Syst.* **1**, 649–707 (1987).

[41] J. D. C. Little, A proof for the queuing formula $L = \lambda W$, *Oper. Res.* **9**, 383–387 (1961).

[42] H. Wielandt, Unzerlegbare, nicht negative Matrizen, *Math. Z.* **52**, 642–648 (1950).

[43] B. S. Tsirelson, Quantum generalizations of Bell's inequality, *Lett. Math. Phys.* **4**, 93–100 (1980).

[44] A. Fine, Hidden variables, joint probability, and the Bell inequalities, *Phys. Rev. Lett.* **48**, 291–295 (1982).

[45] J. F. Clauser, M. A. Horne, A. Shimony and R. A. Holt, Proposed experiment to test local hidden-variable theories, *Phys. Rev. Lett.* **23**, 880–884 (1969).

[46] J. S. Bell, On the Einstein Podolsky Rosen paradox, *Physics* **1**, 195–200 (1964).